Deep genetic divergence in the Deep South: An integrative approach to species delimitation reveals the paraphyletic nature of speciation in the trapdoor spider genus *Cyclocosmia*.

by

Kellie Catherine Bourguignon

A thesis submitted to the Graduate Faculty of
Auburn University
in partial fulfillment of the
requirements for the Degree of
Master of Science

Auburn, Alabama
May 5, 2018

Key words: integrative approach, species delimitation, paraphyletic speciation, mygalomorph spider, niche modeling, *Cyclocosmia*

Approved by

Jason Bond, Chair, Professor and Chair of the Department of Biological Sciences
Johnathan Armbruster, Professor of Biological Sciences
Brent Hendrixson, Associate Professor of Biology

Abstract

      Mygalomorph spiders house an incredible amount of cryptic genetic information, making them an excellent model for species delimitation. An integrative approach to species delimitation uses multiple lines of evidence to increase objectivity and greater accuracy. We apply an integrative approach to the trapdoor spider genus *Cyclocosmia*. Both discovery (concatenation) and validation (Bayes factor delimitation) were used. These methods found strong structuring across the landscape and paraphyletic speciation. The results of these methods contrasted starkly with the morphology, which was supported as two species using a morphometric analysis. Gene flow is an important aspect of speciation and was investigated using the program PHRAPL, which found overall relatively low levels of migration. Niche differences and the projected distributions of these species were calculated using niche based distribution modeling. Based on these integrated methods, the refined hypothesis for this group is three species.

Acknowledgments

I would like to thank the members of the Bond lab and my committee member, Dr. Jason Bond, Dr. Jon Armbruster, and Dr. Brent Hendrixson.

Table of Contents

List of Figures

List of Tables

Chapter 1

Introduction

      With over 47,000 nominal species worldwide, distributed among 113 families (World Spider Catalog, 2017), spiders (order Araneae) rank among the most diverse organisms and are generally held as the largest exclusively predatory animal group. Of the two infraorders, Araneomorphae and Mygamlomorphae, the former contains over 90% of the described species and the vast majority of the morphological diversity. The focus of this study is the mygalomorphs, tarantulas, trapdoor spiders, and their kin (Coddington & Levi, 1991). Mygalomorph morphology is fairly uniform, with bulky bodies and plesiomorphic features such as paraxial chelicerae, two pairs of book lungs, and overall much simpler reproductive organs and silk glands (Raven, 1985).

      Mygalomorph spiders present a special case for understanding evolutionary pattern and process; they tend to be morphologically conserved at both shallow (Jason E. Bond & Stockman, 2008; Hedin & Carlson, 2011; Leavitt, Starrett, Westphal, & Hedin, 2015; Satler, Starrett, Hayashi, & Hedin, 2011; Starrett & Hedin, 2007) and sometimes even deep (Opatova, Bond, & Arnedo, 2013) phylogenetic levels, thus secondary sexual characters traditionally used in spider taxonomy are often uninformative in species recognition and diagnosis. Historically much of the group's higher taxonomic circumscription has been based on morphology, rendering the majority of mygalomorph families (over half) as either paraphyletic or polyphyletic (Jason E. Bond, Hendrixson, Hamilton, & Hedin, 2012). The paucity of diagnostic features at multiple hierarchical levels has led to an increased reliance on molecular approaches (but see below) to understanding the group's evolutionary history particularly at the population-species interface (Jason E. Bond & Hedin, 2006; Jason E. Bond & Stockman, 2008; Hamilton, Formanowicz, & Bond, 2011; Hamilton, Hendrixson, Brewer, & Bond, 2014; Hedin & Carlson, 2011; Hendrixson, DeRussy, Hamilton, & Bond, 2013; Leavitt *et al*., 2015; Montes de Oca, D'Elía, & Pérez-Miles, 2016; Opatova, Bond, & Arnedo, 2016; Satler *et al*., 2011). Further compounding the problem, the non-vagile nature of many mygalomorph species leads to an extreme genetic structuring and cryptic speciation. This pattern was detected by both the sole use of mtDNA markers (Bond *et al.* 2001) and multi-locus data (e.g, Satler *et al.*, 2013; Hamilton *et al.*, 2016),

which makes the group an ideal model system for exploring integrative approaches to delimiting species (Jason E. Bond & Stockman, 2008; Montes de Oca *et al*., 2016), and thanks to their philopatric nature, also biogeography (Opatova *et al*., 2016).

Despite the issues noted above, the vast majority of mygalomorph species are described on the basis of morphological (Bond, 2012); morphology-based delimitation in mygalomorph spiders remains widely used despite the recognized prevalence of species crypsis (Jason E. Bond & Stockman, 2008; Hamilton *et al*., 2014; Hendrixson *et al*., 2013; Leavitt *et al*., 2015; Opatova *et al*., 2016; Satler *et al*., 2013; Stockman & Bond, 2007). Morphological stasis coupled with extreme population-level genetic divergence are further confounded by ambiguity in how species are defined. For example, there are more than 20 species concepts, each emphasizing different aspects of the speciation process (de Queiroz, 2007; Hausdorf, 2011; Mayden, 1997) albeit with the shared characteristic of independence of evolutionary lineages (de Queiroz, 1998; Mayden, 1997). Because most mygalomorph spider species contain deeply diverged populations, by definition considered as independent evolutionary lineages, integrative approaches that evaluate multiple other lines of evidence (e.g., behavioral, morphological, ecological) are sometimes necessary to delimit species in cases where reliance on genetic data alone would likely result in over-splitting (i.e., confuse geographic structuring alone as species boundaries – Sukumaran & Knowles 2017).

Combining multiple lines of evidence and multi-locus or genomic data in an integrative approach increases objectivity and robustness when delimiting species (Carstens, Pelletier, Reid, & Satler, 2013; Edwards & Knowles, 2014; Padial, Miralles, De la Riva, & Vences, 2010). Over the past few decades, advances in, for example, digital imaging, analytical approaches to evaluating morphological shape space, and niche based distribution modeling, have facilitated empirical approaches to quantitatively comparing populations and species. However, until recently (Hamilton *et al*., 2016; Starrett *et al*., 2017) large scale multi-locus nuclear markers had not been developed for use in mygalomorph spiders thereby limiting the genetic scope of addressable questions. Next generation sequencing based methods like Anchored Hybrid Enrichment (Lemmon, Emme, & Lemmon, 2012) and Ultra Conserved Elements (Faircloth *et al*., 2012) that are able to generate large numbers of nuclear loci are especially applicable to non-

2

model organisms like spiders. Moreover, these large datasets capitalize on species delimitation methods that use multi-locus coalescent-based approaches (Fujita, Leaché, Burbrink, McGuire, & Moritz, 2012; A. Leaché & Fujita, 2010) where gene flow and other demographic measures can be estimated as part of the process.

Despite the demonstrated efficacy of approaches to species delimitation that use multiple lines of evidence and genomic data, the point at which two populations qualify as species is seldom clear-cut. For example, the stochastic process of lineage sorting results in a species ontology where loci will appear polyphyletic and then paraphyletic before sorting to genealogical exclusivity (Powell, 1991; Takahata & Slatkin, 1990). Consequently, genetic patterns of non-monophyly could be indicative of incipient speciation despite the fact that some authors maintain that species, by definition, cannot be paraphyletic (Mayden, 1997). However, patterns that show speciation where lineages remain paraphyletic have been found to be fairly common in groups like birds (Omland, Tarr, Boarma, Marzluff, & Fleischer, 2000; Päckert & Martens, 2008; Salzburger, Martens, & Sturmbauer, 2002), plants (Crisp & Chandler, 1996; Good-Avila, Souza, Gaut, & Eguiarte, 2006; Shaw & Allen, 2000; Thulin, Thiede, & Liede-Schumann, 2012), insects (Lukhtanov, Sourakov, Zakharov, & Hebert, 2009; Pons *et al.*, 2006), and spiders (Hendrixson & Bond, 2005a); species paraphyly has been detected at a relatively high rate in the literature (Funk & Omland, 2003). Paraphyletic speciation often appears when there is cryptic diversity, and the phenomenon occurs when cryptic species are more genetically related to another described species than the species with which it shares morphological similarity (Funk & Omland, 2003).

The objective of this study is to explore species delimitation in the putatively closely related members of the trapdoor spider genus *Cyclocosmia* (Araneae: Mygalomorphae: Centizidae). Like other mygalomorph spider species, preliminary mtDNA-based studies of *Cyclocosmia* (unpublished) indicated a pattern of strong genetic structuring and species paraphyly. We use an integrative approach to make informed decisions regarding species boundaries in these taxa. We employ hundreds of loci and coalescent-based methods to genetically evaluate population structuring and gene flow across two geographically restricted North American species. The genomic-based results are then integrated with morphometry and niche based distribution modeling to evaluate morphological and ecological difference between

the putative lineages. The results confirm a pattern of deep geographic structuring and paraphyletic morphological divergence. Although the multi-locus species delimitation results are suggestive of numerous additional species, an integrative approach evaluating presence of gene flow and the results of niche based distribution modeling and morphological analysis is used to make informed decisions regarding species boundaries in these taxa.

The Study System

Cyclocosmia species have a geographically disjunct distribution, known only from eastern Asia (China and Thailand) and in North America (United States and Mexico) (Gertsch & Platnick, 1975; World Spider Catalog, 2017). The genus can be easily identified by a sclerotized, truncated, disc shaped abdominal modification covered in ridges and grooves, the edge of which is rimmed with thick hairs (Fig. 1). Species descriptions for the genus are based primarily on the variation of this hardened, plate-like structure (Gertsch & Platnick, 1975; Schwendinger, 2005; Xu, Xu, Li, Dinh-Sac, & Li, 2017). This modification is most likely used in defense against common predators, such as parasitic wasps, where the abdomen acts as a shield, potentially providing protection from an invader when *Cyclocosmia* retreats headfirst into the burrow (Gertsch & Platnick, 1975).

Two of the eight species in the genus are from the southeastern United States: *C. truncata* (Hentz, 1841), which is found throughout much of Alabama, central-southern Tennessee, and northwestern Georgia, and *C. torreya* (Gertsch & Platnick, 1975), which is found in southwestern Georgia and northwestern Florida (Fig. 2). The secondary sexual characteristics are homogeneous for these two species (Gertsch & Platnick, 1975). The most notable differences are in the rim of the truncation, which is a raised margin around the truncated abdominal disc with gaps along the outside of the disc. The rim is more protruding in *C. torreya* than in *C. truncata*, and there is generally a difference in the pattern of gaps along the ventral edge (Fig. 1). Setae projecting off the rim are more numerous in *C. torreya* and the number of ribs on the truncation is slightly higher in *C. truncata*. The diagnostic differences between these species appear to be limited to these features of the abdomen (Gertsch & Platnick, 1975).

Methods

DNA Extraction and Sequencing

Specimens were collected throughout most of the known ranges of the species and deposited in the Auburn University Museum of Natural History (AUMNH). Genomic DNA was extracted for all field-collected specimens from the leg tissue using a Qiagen DNeasy Blood & Tissue kit. DNA concentration was evaluated through agarose gel electrophoresis and spectrophotometry using a NanoDrop ND-1000. Individuals sequenced include *C. truncata*, *C. torreya*, and *Cyclocosmia*. sp specimens from China and Thailand listed in Table 1. Given the scarce availability of nuclear markers for non-model organisms, the anchored hybrid enrichment method was applied. Anchored hybrid enrichment uses highly conserved sites flanked by less conserved regions of the nuclear genome to obtain variation and areas to create probes, ideal for investigating deep or shallow divergence times (Lemmon *et al*. 2012).

Data were collected following the general methods of (Hamilton *et al*., 2016) and Library preparation, enrichment, and sequencing were conducted at the Center for Anchored Phylogenomics at Florida State University (www.anchoredphylogeny.com) using probes designed in Hamilton *et al.* (2016) to capture and enrich loci from genomic data. After extraction, up to 500 ng of each DNA sample was sonicated to a fragment size of ~300-800 bp using a Covaris E220 ultrasonicator. Indexed libraries were then prepared following Meyer & Kircher (2010), but with modifications for automation on a Beckman-Coulter Biomek FXp liquid-handling robot (see Hamilton *et al.* 2016 for details). Size-selection using SPRI select beads (Beckman-Coulter Inc.; 0.9x ratio of bead to sample volume) was performed after blunt-end repair. Indexed samples were pooled at equal quantities (16 samples per pool), and then each pool was enriched using the AHE Spider Probe. The enrichment reactions were then sequenced on one PE150 Illumina HiSeq 2500 lane at Florida State University Translational Science Laboratory in the College of Medicine.

Orthology was determined among the homologous consensus sequences at each locus following Prum *et al.* (2015) and Hamilton *et al.* (2016). Sequences were clustered using a Neighbor-Joining algorithm by distance, but allowing at most one sequence per species to be in a given cluster. Sequences in each orthologous cluster were aligned using MAFFT v7.023b (Katoh

& Standley, 2013), using the --genafpair and --maxiterate 1000 flags. The alignment for each locus was then trimmed/masked using the steps described in (Hamilton *et al*., 2016). Following the targeting of the 585 loci in the Spider Probe Kit, 601 loci were recovered for 17 ingroup specimens and six outgroup specimens. The result of more loci than targeted occurs when, as part of the bioinformatics pipeline, probed loci with low coverage after alignment are separated into individual loci.

Phylogenetic Analyses

The resulting loci were aligned using MAFFT 7.309 (Katoh & Standley, 2013) and alignment editing was performed using Aliscore 2.2 (Kück *et al*., 2010; Misof & Misof, 2009) and Alicut 2.3. Sequences with no missing data and one allele per individual were concatenated into a supermatrix using FASconCAT-G 1.02 (Kück & Meusemann, 2010). Both maximum likelihood and Bayesian inference analyses were performed on the concatenated supermatrix and were run remotely on the Hopper Cluster at Auburn University. The analyses were rooted with two *Hebestatis theveneti* individuals and two *Ummidia* species (both genera in family Ctenizidae). Partitioning schemes and evolutionary models were selected using PartitionFinder2 (Lanfear, Frandsen, Wright, Senfeld, & Calcott, 2016) using the rcluster algorithm (Lanfear, Calcott, Kainer, Mayer, & Stamatakis, 2014) whith RAxML implementation (Stamatakis, 2014), linked branch lengths, and GTR models of molecular evolution. The concatenated data matrix (367 loci) was partitioned and models assigned as suggested by PartitionFinder2 for each analysis. Maximum likelihood (ML) analyses were performed using RAxML 8.2.9 (Stamatakis, 2014) with 1000 independent searches; the support of the nodes was assessed by 1000 bootstrap replicates. Bayesian inference (BI) analyses were conducted in ExaBayes 1.4.1 (Aberer, Kobert, & Stamatakis, 2014). Two independent runs of 50 million generations with 4 MCMC (Markov Chain Monte Carlo) chains each were run starting from a parsimony starting tree and resampling every 1,000 generations.

Multispecies Coalescent and Bayes Factor Species Delimitation

In Bayes factor species delimitation (BFD), marginal likelihoods are estimated for predetermined speciation hypotheses and are subsequently compared using Bayes factors. In each model, the individuals are assigned into lineages (putative species) according to the

hypothesis that is being tested. The best performing model, indicated by the model with the highest marginal likelihood value, identifies the number of lineages and assignment of individuals to lineages that best explain the data. BFD has been shown to perform well when compared to other coalescent-based species delimitation methods (Grummer, Bryson, & Reeder, 2014; A. Leaché & Fujita, 2010) and also performs well with low sample sizes (A. D. Leaché, Fujita, Minin, & Bouckaert, 2014). This method has the advantage of not needing a guide tree, which can bias Bayesian species delimitation when incorrect (A. Leaché & Fujita, 2010), and can therefore test non-nested models (Grummer *et al*., 2014).

Six competing species delimitation models were generated based on current taxonomic groupings and results of the maximum likelihood and Bayesian inference (see Results, Fig. 3). Groups for the morphology hypothesis are based on morphological species descriptions. Groups for the second, third, and fourth hypotheses were chosen corresponding to the major clades recovered on the concatenated tree (Fig. 3), with three species, four species, and six species, respectively, corresponding to increasing levels of diversity. The fifth is a split hypothesis where every locality, or neighboring localities (less than 20 km apart, 14 species total), is defined as a species. The rearrange hypothesis is a nonsensical hypothesis where individuals of *C. truncata* were reassigned to *C. torreya* lineages and conversely. The split hypothesis and the rearrange hypotheses were tested to evaluate the performance of this method (Grummer *et al*., 2014). Graphical depictions of species delimitation models are shown in Figure 4.

The multi-gene coalescent approach as implemented in *BEAST (Heled & Drummond, 2010) was used to estimate the species-tree for the species delimitation models using the *BEAST package. Due to the computational limitations of BEAST, it was not realistic to conduct the analyses on the entire dataset (415 loci), therefore we analyzed ten sets of 50 randomly selected loci (following Morales *et al.* 2017). The analyses were rooted with a *Cyclocosmia* individual from Thailand based on the results of the full dataset (see below). All North American *Cyclocosmia* individuals (with two alleles each) previously analyzed were included in the analyses and were assigned into lineages (putative species) according to the respective species delimitation model tested.

Two independent runs for each species delimitation model were run for 200 million generations, sampling every 10,000 steps. Computationally less demanding HKY+G nucleotide substitution rate model was assigned to each partition in order to facilitate convergence and to reduce computational effort. Convergence between runs and mixing within each run were visualized with Tracer v1.6 (Rambaut, Suchard, Xie, & Drummond, 2014) to ensure effective sample sizes (ESSs) were greater than 200 after a burn-in of 20%. Individual runs were combined and in LogCombiner (Bouckaert *et al*., 2014). The first 20% of the generations of each run was discarded as burn-in and a consensus tree was inferred with TreeAnnotator (Bouckaert *et al*., 2014).

The species delimitation models were compared using Bayes factor delimitation (BFD) for each of the ten sets of loci. BFD is used to compare species delimitation models using estimated marginal likelihoods. The marginal likelihood for each of the six models (Fig. 4) was estimated with path sampling (Lartillot & Philippe, 2006), implemented in BEAST with two independent runs each for each model in each of the ten sets of loci. The path sampling analysis was run for 50 steps and 1 million iterations for each step. The resulting marginal likelihood values were averaged between the two runs for each model. Bayes factors were calculated as twice the difference in marginal likelihood of two compared models (Kass & Raftery, 1995).

Model Selection and Parameter Estimation with PHRAPL

The program PHRAPL (Jackson, Morales, Carstens, & O'Meara, 2017) estimates divergence and geneflow simultaneously by calculating the statistical fit of models. PHRAPL includes model parameters for both migration and divergence, which are estimated along with model fit. These values are then averaged across all models and used to calculate a genealogical divergence index (gdi; Jackson *et al*. 2017), a value for delimiting species. The maximum number of groups feasibly tested by PHRAPL is four, so individuals in *C. torreya* were assigned to north and south clades (as labeled in Figure 3) to reduce computational time and complexity of the models tested, resulting in three groups. Input gene trees were generated with RAxML using 415 loci, including all North American *Cyclocosmia* individuals and rooted with the *Cyclocosmia* individual from Thailand. Gene trees were generated separately for the north and

south clades with 1000 independent searches with a GTR+G model and rapid hill-climbing algorithm.

Multiple model sets were generated in an effort to reduce the total number of models tested and to simultaneously examine models as complex as possible. Two consecutive model sets were tested, the results of the first used to constrain the second. Only trees with fully resolved topologies were considered in both sets. The model sets tested include 813 total models. The first set included 768 models, with one free parameter given to asymmetric migration (unidirectional or bidirectional migration allowed) and contained all possible combinations of possible topologies. The second set contained 45 models with the same coalescence and migration patterns as the top three models from the first set, with two free parameters given to asymmetric migration, in order to determine the presence of varying levels of migration.

Using PHRAPL, gene trees were subsampled, taking two alleles per group with 100 replicates. The log-likelihood (lnL) and AIC of each model was calculated based on the proportion of matches between simulated and empirical trees, with 100,000 trees simulated for each model and three replicate runs. Simulation of gene trees was conducted using a grid of default parameter values for both population divergence (τ) and migration (m), intended to encompass the full range of potential values. Parameters were averaged over all models and genealogical divergence index (gdi; Jackson *et al.* 2017) values were calculated to determine the level of speciation. Gdi uses divergence times and rates of gene flow to estimate the overall genetic divergence between two taxa. To help interpret cases where reproductive isolation has developed recently and gene flow is detected but in small amounts, the index considers the spatial direction and amount of gene flow present to delimit species instead of simply the presence or absence of gene flow.

Morphological analysis

Specimens were borrowed from the American Museum of Natural History (AMNH). These specimens, along with those in the AUMNH collection (49 specimens total), were used in a morphological analysis. Measurements include carapace length and width, sternum length and width, anterior median eye (AME) separation, posterior median eye (PME) separation, AME-PME separation, and length of the tibia, metatarsus, and tarsus on leg I and IV.

Additionally, two traits unique to the *Cyclocosmia* genus were measured. The length and width of the abdominal disc were measured to detect differences in the shape of the disc. Abdominal disc length was measured from the dorsal to ventral edge of the disc, starting ventrally between the two median ribs running dorsoventrally and ending at the most ventral point. Width of the disc was measured at the widest point of the disc. The length of the margin protrusion was measured due to the seeming variability between the two species. This length was measured from the rib angle (Gertsch & Platnick, 1975) beginning at the edge of the abdominal disc to the tip. The rib angle of the leftmost median ribs running dorsoventrally was measured for each specimen. Only adult female measurements are reported; *C. truncata* males examined showed no difference in palps and no discernable pattern in the spines of the first leg There were no *C. torreya* males available for examination. Spermathecae examined also showed no differences. A principal component analysis (PCA) of log-transformed measurements was conducted and visualized in the statistical program R v3.2.3 (R Core Team, 2015) using the ggbiplot package (Vu, 2011) to find separation of the species in morphological space. Specimens not included in the genetic analysis were assigned to groups for the PCA if they had the same locality as or were adjacent to a locality of a specimen used in the genetic analysis.

Niche Based Distribution Modeling

Using presence only data, niche based distribution modeling estimates the potential ranges of organisms. Environmental data (climate layers) and species distribution data are used to predict the relative stability of habitat and the geographic distribution of the species in the past, present, or future. Species' distributions can then be compared statistically for overlap, which allows to assessment of their potential ecological interchangeability (having similar ecological attributes; Crandall *et al.* 2000).

The potential geographic ranges of the three clades of three species hypothesis and six species hypothesis (Fig. 4) were inferred using the maximum entropy algorithm implemented by Maxent 3.3.3k (Phillips, Anderson, & Schapire, 2006). Coordinates of specimens not included in the genetic analysis were assigned to groups for the distribution modelling if they were adjacent to a locality of a specimen used in the genetic analysis. The 19 bioclimatic layers in 30 arc-second resolution and a digital elevation model were downloaded from WorldClim database

(www.worldclim.org, (Hijmans, Cameron, Parra, Jones, & Jarvis, 2005)) and cropped in ArcGIS version 10 (ESRI) to a range of 29.5°N to 37°N and -82°W to -89°W in order to include the entire known range of *C. truncata* and *C. torreya* (species ranges in Fig. 2). Correlation matrices were generated between the cropped layers in ArcGIS and highly correlated (r>0.85, (Camargo, Werneck, Morando, Sites, & Avila, 2013)) layers were removed, retaining the most biologically informative layer from each correlated group. The 13 remaining bioclimatic layers (BIO2 – Mean Diurnal Range, BIO3 – Isothermality, BIO4 – Temperature Seasonality, BIO5 – Max Temperature of Warmest Month, BIO6 – Min Temperature of Coldest Month, BIO8 – Mean Temperature of Wettest Quarter, BIO9 – Mean Temperature of Driest Quarter, BIO12 – Annual Precipitation, BIO15 – Precipitation Seasonality, BIO16 – Precipitation of Wettest Quarter, BIO17 – Precipitation of Driest Quarter, BIO18 – Precipitation of Warmest Quarter, BIO19 – Precipitation of Coldest Quarter) and the digital elevation model were used for niche based distribution modeling. Species-specific tuning was done to enhance model performance (Anderson & Gonzalez, 2011), and was explored by varying the value of the regularization parameter (0.1, 0.5, 1, 1.5, 2, 3, 4) with autofeatures selected. The model performance was evaluated statistically using the area under the curve (AUC) of the receiver operating characteristic (ROC) plot, which is a threshold-independent measure of model performance as compared to null expectations. Subsequently a set of final analyses were run with 10 replicates for each species group recovered in species delimitation modeling, using the cross-validation testing procedure recommended for enhancement of performance on small datasets (Phillips & Dudík, 2008). The point-wise means of the replicates were used to visualize the distribution models and for further hypothesis testing.

The niche overlap was assessed with the relative rank (RR) metric (Warren & Seifert, 2011) to test the potential ecological interchangeability (Rader, Belk, Shiozawa, & Crandall, 2005) of *Cyclocosmia* species. To evaluate if the overlap values for species pairs are more different than expected if they are drawn from the same underlying distribution, the niche identity test was used with 100 randomized pseudoreplicates to generate a null distribution. The observed overlap was compared to the null distribution with a one-tailed nonparametric test to determines if the distribution models are significantly different from random by comparing the

observed RR to the null distribution. Both niche overlap and identity tests were performed using ENMTools 1.3.3 (Warren, Glor, & Turelli, 2010).

Results

Phylogenetic Analyses

The final concatenated matrix resulted in 176,604 characters sequenced for 23 individuals. Maximum likelihood and Bayesian analyses recovered identical tree topologies, shown in Figure 3. Two nodes with low ML bootstrap support (<80%) had high Bayesian PP support (≥0.99). All other nodes had high bootstrap and posterior probability values. *Cyclocosmia truncata* was recovered as paraphyletic, with *C. torreya* nested within *C. truncata*. *Cyclocosmia truncata* was divided into two well-supported main groups, a northern clade and a southern clade (labeled in Fig. 3). The southern *C. truncata* clade was recovered as sister to a monophyletic *C. torreya* clade. There is well-supported structure within all clades, with geographically proximate localities always recovered as closely related to each other (Fig. 3).

Mutispecies Coalescent and Bayes Factor Delimitation

The ten sets 50 loci yielded an average of 31724 bp for 18 individuals with two alleles each. The *BEAST analyses for the six species hypothesis showed high support for the majority of nodes (Appendix 2). The position of *C. torreya* was not stable across the obtained topologies (Fig. 6); however, its position matched the concatenated dataset (i.e. sister to southern *C. truncata* lineages) in 6 different sets. Alternatively, *C. torreya* was recovered as sister to all *C. truncata* lineages (in three sets), or sister to northern *C. truncata* lineages (one set).

The six species hypothesis (Fig. 4) received the highest marginal likelihood score, so Bayes factors were calculated comparing it to all other models (Table 2). Bayes factors greater than 10 indicate decisive support for one model over the other (Kass & Raftery, 1995), indicating the six species model was strongly supported over the other models in all analyses employing different sets of loci.

Model Selection and Parameter Estimation with PHRAPL

The results of the grid search indicate that a moderate amount migration is present bidirectionally between the north and south clades of *C. truncata* and unidirectionally to *C.*

12

torreya from the north and south clades. There is no inference of migration from *C. torreya* back to either *C. truncata* clade.

For the first model set, the highest supported model (average wAIC=0.966) includes bidirectional migration between the north and south *C. truncata* clades and unidirectional migration from the north and south *C. truncata* clades to *C. torreya* before the first coalescent event (Fig. 7). Bidirectional ancestral migration after the first coalescent event is also present in this model. The overall pattern of migration in the best model of the first set (exclusion of migration from *C. torreya* before the first coalescent event) was used to constrain the second set of models.

Two similar models combined contained most of the wAIC (combined average=0.955) for the second set of models. These models have a higher migration rate after the first coalescent event, with a single migration rate (average wAIC=0.697) or a higher migration rate from the north clade to the south clade (average wAIC=0.257) before the first coalescent event (Fig. 7).

The average gdi value was relatively high (0.66), indicating that these lineages are trending towards genetic divergence. Based on averages for all organisms, a gdi value of 0.20 or below indicates the lineages are not species, while a value of 0.70 or higher indicates distinct species (Jackson, Carstens, *et al*., 2017). The gdi value and the parameter estimates indicate divergence with gene flow. The model averages for τ showed a shallow divergence time between *C. truncata* south and *C. torreya* (~0.58) and a moderate divergence time between ancestral south-*torreya* and *C. truncata* north (~2.7). Migration model averages revealed relatively small migration rates (~0.29 and ~0.86) where migration was present.

Morphology

The PCA (Fig. 5) of the measured morphological characteristics showed a difference between *C. truncata* and *C. torreya*. There was no difference between the lineages within *C. truncata* following the three species hypothesis (Fig. 5a) or the six species hypothesis (Fig. 5b). that the species were separated along PC1, which is most strongly and positively affected by the length of the margin protrusion (described as rib angle and a key difference between the species by Gertsch & Platnick (1975), explaining 80% of the variation in the data. Measurements presented in Appendix 1.

Niche Based Distribution Modeling

Species specific tuning of the beta parameter suggested that the default value of 1 be used for all models. The niche based distribution models performed well for the north (AUC = 0.844, SD = 0.126) and south (AUC = 0.912, SD = 0.092) clades; the species groups supported by the six species hypothesis (Fig. 4), *truncata* 1 (AUC = 0.822, SD = 0.053), *truncata* 2 (AUC = 0.984, SD = 0.010), *truncata* 3 (AUC = 0.905, SD = 0.074), and *truncata* 4 (AUC = 0.876, SD = 0.213); and *C. torreya* (AUC = 0.908, SD = 0.184). Too few data points prevented *truncata* 5 from being included in niche based distribution modeling; at least three are required, but only two were available. Point-wise means from replicate runs were used to visualize the resulting predicted ranges (Fig. 8).

Results from the analysis of variable contributions indicate that isothermality (north clade), the minimum temperature of coldest month (south clade, *truncata* 1, and *C. torreya*), the mean temperature of wettest quarter (*truncata* 2), and the mean temperature of driest quarter (*truncata* 3 and *truncata* 4) contributed the most to the distribution of each group. The null hypothesis that groups shared the same niche model was rejected by pairwise niche-identity tests when significant: observed niche similarities among the species pairs were significantly lower than their randomized null distributions for all pairs except *truncata* 1 and *torreya* (Table 3). Niches were interchangeable for pairs with a significant difference, and not interchangeable for pairs with an insignificant difference. For RR, values near one are considered identical or highly interchangeable and values near zero indicate different niches or non-interchangeability.

Discussion

Accurate species delimitation and subsequent identification is essential for our understanding of biodiversity and it is of a critical importance in conservation efforts (Agapow *et al*., 2004; Isaac, Mallet, & Mace, 2004; Mace, 2004). Delimiting species can be challenging, especially when different lines of evidence do not support the same outcome (e.g., Roe & Sperling 2007); cryptic species may lack morphological differentiation but show deep genetic divergences or different ecological preferences (Opatova *et al*., 2016). Disentangling population structuring within a species from cryptic diversity is a particularly difficult in non vagile groups

14

that are prone to showing deep genetic structuring even in the absence of geographic barriers (Irwin, 2002), and has been a long-standing problem in mygalomorph taxonomy (Jason E. Bond & Stockman, 2008; Montes de Oca *et al*., 2016).

Our multi-locus phylogenetic analyses of *Cyclocosmia* populations show a pattern of strong geographic structuring across the landscape. Morphological divergence appears to be isolated to *C. torreya* populations which render *C. truncata* paraphyletic. Despite the observed morphological homogeneity across *C. truncata* populations, Bayes factor delimitation (BFD) inferred numerous cryptic species. However, molecular model-based analyses show evidence of gene flow between clades and we observed no consistent pattern of ecological divergence corresponding to species indicated by BFD. Based on these results and our discussion below, we conclude there are three species of *Cyclocosmia* in the southeastern United States, one of which is new to science.

The results of our phylogenetic analysis of the concatenated dataset comprising all 367 loci recovered *C. truncata* as paraphyletic with respect to *C. torreya*, violating the expectation of genealogical exclusivity required by some species concepts (de Queiroz, 2007) in these two nominal species. In general, the process of speciation often initially produces paraphyletic lineages that eventually become monophyletic over time (Powell, 1991; Takahata & Slatkin, 1990); paraphyly in the *C. truncata* lineages could be thus indicative of the earlier stages of divergence, which is also supported according to the parameter estimation by PHRAPL (see below). Paraphyly has been detected in other mygalomorphs with a substantial amount of species diversity not captured by morphological methods (Hendrixson & Bond, 2005a), but given the pronounced morphological divergence of *C. torreya* we might anticipate monophyly at some point in the future.

Cyclocosmia truncata populations were also highly structured across the landscape in the concatenated supermatrix. Phylogeographic structure has been shown to increase as vagility decreases and genetic breaks can appear even in continuously distributed species with no physical barrier to gene flow (Irwin, 2002).The low vagility and consequent minimal rate of gene flow create a high potential for population subdivision in mygalomorph spiders (Hendrixson & Bond, 2005a; Hendrixson *et al*., 2013; Leavitt *et al*., 2015; Satler *et al*., 2013, 2011; Starrett &

Hedin, 2007; Stockman & Bond, 2007). It is, therefore, not surprising that an abundance of genetic structuring and hypothesized cryptic species were found within *C. truncata* using the BFD approach.

Despite considerable structuring and genetic divergence, there is no morphological support for the six putative species delimited by BFD. Our morphological analysis did show obvious differences in abdominal morphology between *C. truncata* and *C. torreya* (*sensu* (Gertsch & Platnick, 1975), but none within *C. truncata* (Fig. 5); that is, *C. truncata* populations all appear to be morphologically similar. These results are further supported by additional characters not included in our study (ventral edge of the truncation and number of setae and ribs (Fig. 1) used in the original species' description (Gertsch & Platnick, 1975). The lack of morphological variation would thus support the two species hypothesis when basing species delimitation on morphology alone; however, this particular hypothesis was the lowest ranked BFD hypothesis.

The six candidate species hypothesis is only partially supported using niche based distribution modeling. The relative rank (RR) values of the niche identity test for the comparisons of the candidate species found by BFD (six species hypothesis, Fig. 4) are relatively high, ranging from 0.683 to 0.728 in the geographically adjacent groups (values near 1 indicate niche similarity); however, all pair comparisons but one were significantly lower than the null distribution (Table 3). Conversely, the RR values for the species pairs from the three species hypothesis (Fig. 4), i.e. north clade, south clade, and *C. torreya*, were lower – 0.575 and 0.577 for the adjacent groups (Table 3) and all comparisons of the three species hypothesis were statistically significantly lower than their null distributions (Table 3). The significance indicates that the distribution models for the group pairs were more different than expected than if they were drawn from the same underlying distribution, i.e. their niches are not interchangeable. Despite the statistical difference between the species' niches, overlap values were still moderately high for many geographically adjacent pairs (0.575 to 0.728; Table 3), and considerable overlap between many of the groups tested in the six species hypothesis, especially between *truncata* 1, *truncata* 2, and *truncata* 3 (Fig. 8, bottom a, b, and c) can be assessed visually. There is considerably less overlap in the groups in the three species hypothesis (Fig. 8,

top). It should be noted that niche based distribution modeling accuracy is dependent on the number of presence points (Lozier, Aniello, & Hickerson, 2009; Pearson, Raxworthy, Nakamura, & Peterson, 2007), which in some cases, particularly in the six species hypothesis, were very few for some clades. For example, *truncata* 1 had only three presence points, *truncata* 2 had four, and the north *C. truncata* clade had the most at thirteen. Thus, the range predictions subsequently used for niche overlap assessment might not be accurate.

Molecular species delimitation methods are prone to over-splitting in dispersal limited taxa particularly when they are based on single locus mitochondrial data (Hamilton *et al*., 2014; Hendrixson *et al*., 2013; Leavitt *et al*., 2015; Opatova & Arnedo, 2014). Inadequately delimited species can present problems for conservation related decisions, particularly when small isolated populations are delimited based solely on genetic divergences (Frankham *et al*., 2012). Over-splitting can also mislead total biodiversity metrics (Isaac *et al*., 2004). A recent study has shown that species delimitation methods implementing the multi-species coalescent approach may distinguish between within-species population structure, not species boundaries (Sukumaran & Knowles, 2017). A split hypothesis (Fig. 4) for our data was evaluated using BFD to address this issue and potentially address the concern that it would not drastically overestimate the number of species. This hypothesis obtained low support and the six species hypothesis was preferred instead; however, BFD does not consider gene flow and the preferred six species hypothesis could thus still overestimate *Cyclocosmia* diversity. In simulation testing in the similar species delimitation method BP&P (Yang, 2015), gene flow between non-sister taxa inhibits the ability of Bayesian methods to recover the correct species tree, especially when paraphyletic speciation is present (Leaché *et al.*, 2014b, but see Zhang *et al.*, 2011). Thus, when compared with other evidence (see below), we conclude that the structure found in the highest supported hypothesis by BFD (six species hypothesis, Fig. 4) likely represents intraspecific population structure due to genetic isolation, and not species boundaries.

When we considered the potential for gene flow for our data, fewer species are delimited when compared to the BFD approach. Although not included in most molecular species delimitation methods, gene flow has a homogenizing effect on the genetic divergence associated with speciation. Nevertheless, species diverge in the presence of gene flow (Hey, 2006; Pinho &

Hey, 2010) and has been demonstrated in a variety of taxa (e.g., Jónsson *et al.* 2014; Oliveira *et al.* 2015; Schield *et al.* 2015; Supple *et al.* 2015). We used the program PHRAPL (Jackson, Morales, et al., 2017) to test the fit of different demographic models to the given gene trees and species or population assignments across our *Cyclocosmia* populations. The average gdi value for *Cyclocosmia* (0.66) is just below the empirically determined threshold for species (0.70, Jackson *et al.* 2017), thus the clades tested (three species hypothesis, Fig. 4) might be cautiously interpreted as different species.

The PHRAPL analysis revealed a moderate level of migration within *C. truncata* and unidirectionally from *C. truncata* to *C. torreya*. Overall levels of migration in this system are relatively low, which can indicate recently developed reproductive isolation (Jackson, Carstens, *et al.*, 2017). No migration was detected from *C. torreya* back to *C. truncata*. The low level of migration may represent a case where morphological differences are starting to accrue in the absence of gene flow. Males are known to travel short distances in search of females during mating seasons in other mygalomorph spiders (Bond *et al.*, 2001), but specifics about migration patterns in *Cyclocosmia* are unknown. Therefore, it is possible that males may connect *Cyclocosmia* populations that would be otherwise isolated. The rate of this exchange is presumably small and limited by distance, resulting in the small migration rate detected by PHRAPL and the pattern of migration found. *Cyclocosmia torreya* is relatively geographically isolated from the *C. truncata* clades and has a comparatively reduced range (see light blue range, Fig. 2). Limited mobility may correlate with a reduced range, leading to no migration from *C. torreya* to *C. truncata*.

In addition to genetic, morphological, and ecological evidence, a temporal difference in mating seasons between *C. truncata* and *C. torreya* may act as a gene flow barrier. *C. truncata* males move in the fall (August to November) and *C. torreya* males appear to move in the spring/summer (April to July); all based on museum collection records. There are also potential dispersal timing differences within *C. truncata*. The north clade trends towards the end of the season (October/November) whereas the south clade tends to move at the beginning (August/September), but there is no distinct separation in timing between these groups. The difference in timing could be viewed as a reproductive isolation mechanism because females

may not be receptive to mating when males of another species are active. It has been used as evidence for species delimitation in the mygalomorph spider genus *Antrodiaetus* (Hendrixson & Bond 2005a) (Hendrixson & Bond 2005a); character displacement in body size as well as male dispersal appear to reinforce species boundaries for *A. unicolor* and *A. microunicolor*. The level of gene flow detected by PHRAPL reflects this pattern of reproductive isolation, with low levels of unidirectional gene flow from *C. truncata* to *C. torreya*.

The methods presented here represent an integrative approach to species delimitation, employed in an effort to determine species boundaries within a morphologically conserved group of trapdoor spiders. Morphological homogeneity across these populations of *Cyclocosmia* belies a rich genetic diversity across the landscape. Given the results of these multi-locus analysis and niche based modeling as well as the timing of male dispersal, we conclude there are three species of US *Cyclocosmia*: *C. torreya*, *C. truncata*, and a new species. Our analyses confirm that *C. torreya* is a species, but renders *C. truncata sensu lato* paraphyletic. Most of the structuring identified by BFD is likely population level divergence/structuring, rather than speciation. There is evidence for ecological differentiation for these three species, as well as low gene flow accounted for based on moderately high gdi values.

Multiple lines of evidence (using an integrative approach) indicate cryptic speciation within *C. truncata*; however, not all of the methods we employed converge on the same solution. Genetic methods are needed to inform species delimitation in morphologically conserved groups such as *Cyclocosmia*, where a large amount of genetic divergence was revealed in a morphologically homogenous group. Phylogenetic based analyses like BFD taken alone may be misleading with respect to the number of species they indicate should be delimited. These analyses also seem to be contingent upon the number of loci used and which ones are chosen (Fig. 6; Morales *et al.*, 2017). In our example, disregarding the potential for gene flow seemed to over-split populations of species. Simply relying on researcher intuition to determine demographic models to be tested leads to biased results; reanalysis of datasets using PHRAPL by Carstens *et al.* (2017) often resulted in selection of a model that was not initially included, most often including gene flow. Clearly, considering gene flow is necessary to prevent the oversimplification of model space being tested and possibly ignoring the best model. Ecology

influences the process of speciation, such as through processes that cause vicariance events which in turn facilitate speciation, and niche data can help inform the validity of potential species. Our results further support the fact that a variety of information from diverse sources is needed to best estimate the number of species present (Carstens *et al*., 2013; Edwards & Knowles, 2014; Padial *et al*., 2010).

Works Cited

Aberer, A. J., Kobert, K., & Stamatakis, A. (2014). ExaBayes: Massively Parallel Bayesian Tree Inference for the Whole-Genome Era. *Molecular Biology and Evolution*, *31*(10), 2553–2556.

Agapow, P.-M., Bininda-Emonds, O. R. P., Crandall, K. A., Gittleman, J. L., Mace, G. M., Marshall, J. C., & Purvis, A. (2004). The Impact of Species Concept on Biodiversity Studies. *The Quarterly Review of Biology*, *79*(2), 161–179.

Anderson, R. P., & Gonzalez, I. (2011). Species-specific tuning increases robustness to sampling bias in models of species distributions: An implementation with Maxent. *Ecological Modelling*, *222*(15), 2796–2811.

Bond, J. E., & Hedin, M. (2006). A total evidence assessment of the phylogeny of North American euctenizine trapdoor spiders (Araneae, Mygalomorphae, Cyrtaucheniidae) using Bayesian inference. *Molecular Phylogenetics and Evolution*, *41*(1), 70–85.

Bond, J. E., Hedin, M. C., Ramirez, M. G., & Opell, B. D. (2001). Deep molecular divergence in the absence of morphological and ecological change in the californian coastal dune endemic trapdoor spider Aptostichus simus. *Molecular Ecology*, *10*(4), 899–910.

Bond, J. E., Hendrixson, B. E., Hamilton, C. A., & Hedin, M. (2012). A reconsideration of the classification of the Spider infraorder mygalomorphae (Arachnida: Araneae) based on three nuclear genes and morphology. *PLoS ONE*, *7*(6).

Bond, J. E., & Stockman, A. K. (2008). An Integrative Method for Delimiting Cohesion Species: Finding the Population-Species Interface in a Group of Californian Trapdoor Spiders with Extreme Genetic Divergence and Geographic Structuring. *Systematic Biology*, *57*(4), 628–646.

Bouckaert, R., Heled, J., Kühnert, D., Vaughan, T., Wu, C.-H., Xie, D., … Drummond, A. J. (2014). BEAST 2: A Software Platform for Bayesian Evolutionary Analysis. *PLoS Computational Biology*, *10*(4), e1003537.

Camargo, A., Werneck, F. P., Morando, M., Sites, J. W., & Avila, L. J. (2013). Quaternary range and demographic expansion of Liolaemus darwinii (Squamata: Liolaemidae) in the Monte Desert of Central Argentina using Bayesian. *Molecular Ecology*, *22*(15), 4038–4054.

Carstens, B. C., Morales, A. E., Jackson, N. D., & O'Meara, B. C. (2017). Objective choice of phylogeographic models. *Molecular Phylogenetics and Evolution*, *116*, 136–140.

Carstens, B. C., Pelletier, T. A., Reid, N. M., & Satler, J. D. (2013). How to Fail at Species Delimitation. *Molecular Ecology*, *22*, 4369–433.

Coddington, J. A., & Levi, H. W. (1991). Systematics and evolution of spiders. *Annual Review of Ecology, Evolution, and Systematics*, *22*(1991), 565–592.

Crandall, K. A., Bininda-emonds, O. R. P., Mace, G. M., & Wayne, R. K. (2000). Considering evolutionary processes in conservation biology. *Trends in Ecology and Evolution*, *15*(7), 290–295.

Crisp, M., & Chandler, G. (1996). Paraphyletic species. *Telopea*, *6*(4), 813–844.

de Queiroz, K. (1998). The General Lineage Concept of Species , Species Crteria , and the Process of Speciation and Terminological Recommendations. In *Endless Forms: Species and Speciation* (pp. 57–75).

de Queiroz, K. (2007). Species Concepts and Species Delimitation. *Systematic Biology*, *56*(6), 879–886.

Edwards, D. L., & Knowles, L. L. (2014). Species detection and individual assignment in species delimitation: can integrative data increase efficacy? *Proceedings of the Royal Society B: Biological Sciences*, *281*(1777), 20132765.

Faircloth, B. C., McCormack, J. E., Crawford, N. G., Harvey, M. G., Brumfield, R. T., & Glenn, T. C. (2012). Ultraconserved Elements Anchor Thousands of Genetic Markers Spanning Multiple Evolutionary Timescales. *Systematic Biology*, *61*(5), 717–726.

Frankham, R., Ballou, J. D., Dudash, M. R., Eldridge, M. D. B., Fenster, C. B., Lacy, R. C., … Ryder, O. A. (2012). Implications of different species concepts for conserving biodiversity. *Biological Conservation*, *153*, 25–31.

Fujita, M. K., Leaché, A. D., Burbrink, F. T., McGuire, J. A., & Moritz, C. (2012). Coalescent-based species delimitation in an integrative taxonomy. *Trends in Ecology and Evolution*, *27*(9), 480–488.

Funk, D. J., & Omland, K. E. (2003). Species-Level Paraphyly and Polyphyly: Frequency, Causes, and Consequences, with Insights from Animal Mitochondrial DNA Insights from Animal Mitochondrial DNA. *Annual Review of Ecology, Evolution, and Systematics*, *34*, 397–423.

Gertsch, W. J., & Platnick, N. I. (1975). A revision of the trapdoor spider genus Cyclocosmia (Araneae, Ctenizidae). *American Museum Novitates*, (2580), 1–20.

Good-Avila, S. V, Souza, V., Gaut, B. S., & Eguiarte, L. E. (2006). Timing and rate of speciation in Agave (Agavaceae). *Proceedings of the National Academy of Sciences of the United States of America*, *103*(24), 9124–9129.

Grummer, J. A., Bryson, R. W., & Reeder, T. W. (2014). Species delimitation using bayes factors: Simulations and application to the sceloporus scalaris species group (Squamata: Phrynosomatidae). *Systematic Biology*, *63*(2), 119–133.

Hamilton, C. A., Formanowicz, D. R., & Bond, J. E. (2011). Species Delimitation and Phylogeography of Aphonopelma hentzi (Araneae, Mygalomorphae, Theraphosidae): Cryptic Diversity in North American Tarantulas. *PLoS ONE*, *6*(10), e26207.

Hamilton, C. A., Hendrixson, B. E., Brewer, M. S., & Bond, J. E. (2014). An evaluation of sampling effects on multiple DNA barcoding methods leads to an integrative approach for delimiting species: A case study of the North American tarantula genus Aphonopelma (Araneae, Mygalomorphae, Theraphosidae). *Molecular Phylogenetics and Evolution*, *71*(1), 79–93.

Hamilton, C. A., Lemmon, A. R., Lemmon, E. M., & Bond, J. E. (2016). Expanding anchored hybrid enrichment to resolve both deep and shallow relationships within the spider tree of life. *BMC Evolutionary Biology*, *16*(1), 212.

Hausdorf, B. (2011). Progress Toward a General Species Concept. *Evolution*, *65*(4), 923–931.

Hedin, M., & Carlson, D. (2011). A new trapdoor spider species from the southern Coast Ranges of California (Mygalomorphae, Antrodiaetidae, Aliatypus coylei, sp. nov,), including consideration of mitochondrial phylogeographic structuring. *Zootaxa*, *68*(2963), 55–68.

Heled, J., & Drummond, A. J. (2010). Bayesian inference of species trees from multilocus data. *Molecular Biology and Evolution*, *27*(3), 571–580.

Hendrixson, B. E., & Bond, J. E. (2005a). Testing species boundaries in the Antrodiaetus unicolor complex (Araneae: Mygalomorphae: Antrodiaetidae): "Paraphyly" and cryptic diversity. *Molecular Phylogenetics and Evolution*, *36*(2), 405–416.

Hendrixson, B. E., & Bond, J. E. (2005b). Two sympatric species of Antrodiateus from southwestern North Carolina (Araneae, Mygalomorphae, Anthropiaetidae). *Zootaxa*, *872*(1), 1–19.

Hendrixson, B. E., DeRussy, B. M., Hamilton, C. A., & Bond, J. E. (2013). An exploration of species boundaries in turret-building tarantulas of the Mojave Desert (Araneae, Mygalomorphae, Theraphosidae, Aphonopelma). *Molecular Phylogenetics and Evolution*, *66*(1), 327–340.

Hentz, N. M. (1841). Species of Mygale of the United States. *Proceedings of the Boston Society of Natural History*, *1*, 41–42.

Hey, J. (2006). Recent advances in assessing gene flow between diverging populations and species. *Current Opinion in Genetics & Development*, *16*(6), 592–596.

Hijmans, R. J., Cameron, S. E., Parra, J. L., Jones, P. G., & Jarvis, A. (2005). Very high resolution interpolated climate surfaces for global land areas. *International Journal of Climatology*, *25*, 1965–1978.

Irwin, D. E. (2002). Phylogeographic Breaks without Geographic Barriers to Gene Flow. *Evolution*, *56*(12), 2383–2394.

Isaac, N. J. B., Mallet, J., & Mace, G. M. (2004). Taxonomic inflation: Its influence on macroecology and conservation. *Trends in Ecology and Evolution*, *19*(9), 464–469.

Jackson, N. D., Carstens, B. C., Morales, A. E., & O'Meara, B. C. (2017). Species Delimitation with Gene Flow. *Systematic Biology*, *66*(5), 799–812.

Jackson, N. D., Morales, A. E., Carstens, B. C., & O'Meara, B. C. (2017). PHRAPL: Phylogeographic Inference Using Approximate Likelihoods. *Systematic Biology*, *19*, 431–435.

Jónsson, H., Schubert, M., Seguin-Orlando, A., Ginolhac, A., Petersen, L., Fumagalli, M., … Orlando, L. (2014). Speciation with gene flow in equids despite extensive chromosomal plasticity. *Proceedings of the National Academy of Sciences*, *111*(52), 18655–18660.

Kass, R. E., & Raftery, A. E. (1995). Bayes factors. *Journal of the American Statistical Association*, *90*(430), 773–795.

Katoh, K., & Standley, D. M. (2013). MAFFT Multiple Sequence Alignment Software Version 7: Improvements in Performance and Usability. *Molecular Biology and Evolution*, *30*(4), 772–780.

Kück, P., & Meusemann, K. (2010). FASconCAT: Convenient handling of data matrices. *Molecular Phylogenetics and Evolution*, *56*(3), 1115–1118.

Kück, P., Meusemann, K., Dambach, J., Thormann, B., von Reumont, B. M., Wägele, J. W., & Misof, B. (2010). Parametric and non-parametric masking of randomness in sequence alignments can be improved and leads to better resolved trees. *Frontiers in Zoology*, *7*(1), 10.

Lanfear, R., Calcott, B., Kainer, D., Mayer, C., & Stamatakis, A. (2014). Selecting optimal partitioning schemes for phylogenomic datasets. *BMC Evolutionary Biology*, *14*(82).

Lanfear, R., Frandsen, P. B., Wright, A. M., Senfeld, T., & Calcott, B. (2016). PartitionFinder 2: new methods for selecting partitioned models of evolution for molecular and morphological phylogenetic analyses. *Molecular Biology and Evolution*, *34*(3), 772–773.

Lartillot, N., & Philippe, H. (2006). Computing Bayes Factors Using Thermodynamic Integration. *Systematic Biology*, *55*(2), 195–207.

Leaché, A. D., Fujita, M. K., Minin, V. N., & Bouckaert, R. R. (2014). Species delimitation using genome-wide SNP Data. *Systematic Biology*, *63*(4), 534–542.

Leaché, A. D., Harris, R. B., Rannala, B., & Yang, Z. (2014). The Influence of Gene Flow on Species Tree Estimation: A Simulation Study. *Systematic Biology*, *63*(1), 17–30.

Leaché, A., & Fujita, M. (2010). Bayesian species delimitation in West African forest geckos (Hemidactylus fasciatus). *Proceedings of the Royal Society B*.

Leavitt, D. H., Starrett, J., Westphal, M. F., & Hedin, M. (2015). Multilocus sequence data reveal dozens of putative cryptic species in a radiation of endemic Californian mygalomorph spiders (Araneae, Mygalomorphae, Nemesiidae). *Molecular Phylogenetics and Evolution*, *91*, 56–67.

Lemmon, A. R., Emme, S. A., & Lemmon, E. M. (2012). Anchored hybrid enrichment for massively high-throughput phylogenomics. *Systematic Biology*, *61*(5), 727–744.

Lozier, J. D., Aniello, P., & Hickerson, M. J. (2009). Predicting the distribution of Sasqua in western North America: anything goes with ecological niche modelling. *Journal of Biogeography*, *36*, 1623–1627.

Lukhtanov, V. A., Sourakov, A., Zakharov, E. V., & Hebert, P. D. N. (2009). DNA barcoding Central Asian butterflies: Increasing geographical dimension does not significantly reduce the success of species identification. *Molecular Ecology Resources*, *9*(5), 1302–1310.

Mace, G. M. (2004). The Role of Taxonomy in Species Conservation. *Philosophical Transactions of the Royal Society B*, *359*, 711–719.

Mayden, R. L. (1997). A hierarchy of species concepts: the denouement in the saga of the species problem. In *Species: The Units of Biodiversity* (pp. 381–423).

Meyer, M., & Kircher, M. (2010). Illumina sequencing library preparation for highly multiplexed target capture and sequencing. *Cold Spring Harbor Protocols*, *5*(6).

Misof, B., & Misof, K. (2009). A Monte Carlo Approach Successfully Identifies Randomness in Multiple Sequence Alignments: A More Objective Means of Data Exclusion. *Systematic Biology*, *58*(1), 21–34.

Montes de Oca, L., D'Elía, G., & Pérez-Miles, F. (2016). An integrative approach for species delimitation in the spider genus Grammostola (Theraphosidae, Mygalomorphae). *Zoologica Scripta*, *45*(3), 322–333.

Morales, A. E., Jackson, N. D., Dewey, T. A., O'Meara, B. C., & Carstens, B. C. (2017). Speciation with gene flow in North American Myotis bats. *Systematic Biology*, *66*(3), 440–452.

Oliveira, E. F., Gehara, M., São-Pedro, V. A., Chen, X., Myers, E. A., Burbrink, F. T., … Costa, G. C. (2015). Speciation with gene flow in whiptail lizards from a Neotropical xeric biome. *Molecular Ecology*, *24*(23), 5957–5975.

Omland, K. E., Tarr, C. L., Boarma, W. I., Marzluff, J. M., & Fleischer, R. C. (2000). Cryptic genetic variation and paraphyly in ravens. *Proceedings of the Royal Society B: Biological Sciences*, *267*, 2475–2482.

Opatova, V., & Arnedo, M. A. (2014). Spiders on a Hot Volcanic Roof: Colonisation Pathways and Phylogeography of the Canary Islands Endemic Trap-Door Spider Titanidiops canariensis (Araneae, Idiopidae). *PloS One*, *9*(12), e115078.

Opatova, V., Bond, J. E., & Arnedo, M. A. (2013). Ancient origins of the Mediterranean trap-door spiders of the family Ctenizidae (Araneae, Mygalomorphae). *Molecular Phylogenetics*

and Evolution, *69*(3), 1135–1145.

Opatova, V., Bond, J. E., & Arnedo, M. A. (2016). Uncovering the role of the Western Mediterranean tectonics in shaping the diversity and distribution of the trap-door spider genus Ummidia (Araneae, Ctenizidae). *Journal of Biogeography*, *43*(10), 1955–1966.

Päckert, M., & Martens, J. (2008). Taxonomic pitfalls in tits - Comments on the Paridae chapter of the handbook of the birds of the world. *Ibis*, *150*(4), 829–831.

Padial, J. M., Miralles, A., De la Riva, I., & Vences, M. (2010). The Integrative Future of Taxonomy. *Frontiers in Zoology*, *7*(1), 16.

Pearson, R. G., Raxworthy, C. J., Nakamura, M., & Peterson, A. T. (2007). Predicting species distributions from small numbers of occurrence records: a test case using cryptic geckos in Madagascar. *Journal of Biogeography*, *34*(1), 102–117.

Phillips, S. J., Anderson, R. P., & Schapire, R. E. (2006). Maximum entropy modeling of species geographic distributions. *Ecological Modelling*, *190*(3–4), 231–259.

Phillips, S. J., & Dudík, M. (2008). Modeling of Species Distributions with Maxent: New Extensions and a Comprehensive Modeling of species distributions with Maxent: new extensions and a comprehensive evaluation. *Source: Ecography*, *31*(2), 161–175.

Pinho, C., & Hey, J. (2010). Divergence with Gene Flow: Models and Data. *Annual Review of Ecology, Evolution, and Systematics*, *41*(1), 215–230.

Pons, J., Barraclough, T. G., Gomez-Zurita, J., Cardoso, A., Duran, D. P., Hazell, S., … Vogler, A. P. (2006). Sequence-based species delimitation for the DNA taxonomy of undescribed insects. *Systematic Biology*, *55*(4), 595–609.

Powell, J. R. (1991). Monophyly / Paraphyly / Polyphyly and Gene/Species Trees: An Example from Drosophila. *Molecular Biology and Evolution*, *8*(6), 892–896.

Prum, R. O., Berv, J. S., Dornburg, A., Field, D. J., Townsend, J. P., Lemmon, E. M., & Lemmon, A. R. (2015). A comprehensive phylogeny of birds (Aves) using targeted next-generation DNA sequencing. *Nature*, *526*, 569–573.

Rader, R. B., Belk, M. C., Shiozawa, D. K., & Crandall, K. A. (2005). Empirical tests for ecological exchangeability. *Animal Conservation*, *8*(April 2017), 239–247.

Rambaut, A., Suchard, M. A., Xie, D., & Drummond, A. J. (2014). Tracer v1.6, Available from http://beast.bio.ed.ac.uk/Tracer.

Raven, R. J. (1985). The spider infraorder Mygalomorphae (Araneae): cladistics and systematics. *Bulletin of the American Museum of Natural History*, *182*, 1–180.

Roe, A. D., & Sperling, F. A. H. (2007). Population structure and species boundary delimitation of cryptic Dioryctria moths: an integrative approach. *Molecular Ecology*, *16*(17), 3617–3633.

Salzburger, W., Martens, J., & Sturmbauer, C. (2002). Paraphyly of the Blue Tit (Parus caeruleus) suggested from cytochrome b sequences. *Molecular Phylogenetics and Evolution*, *24*(1), 19–25.

Satler, J. D., Carstens, B. C., & Hedin, M. (2013). Multilocus Species Delimitation in a Complex of Morphologically Conserved Trapdoor Spiders (Mygalomorphae, Antrodiaetidae, Aliatypus). *Systematic Biology*, *62*(6), 805–823.

Satler, J. D., Starrett, J., Hayashi, C. Y., & Hedin, M. (2011). Inferring species trees from gene trees in a radiation of california trapdoor spiders (Araneae, Antrodiaetidae, Aliatypus). *PLoS ONE*, *6*(9), e25355.

Schield, D. R., Card, D. C., Adams, R. H., Jezkova, T., Reyes-Velasco, J., Proctor, F. N., … Castoe, T. A. (2015). Incipient speciation with biased gene flow between two lineages of the Western Diamondback Rattlesnake (Crotalus atrox). *Molecular Phylogenetics and Evolution*, *83*, 213–223.

Schwendinger, P. J. (2005). Two new Cyclocosmia (Araneae: Ctenizidae) from Thailand. *Revue Suisse de Zoologie*, *112*(1), 225–252.

Shaw, A. J., & Allen, B. (2000). Phylogenetic relationships, morphological incongruence, and geographic speciation in the fontinalaceae (Bryophyta). *Molecular Phylogenetics and Evolution*, *16*(2), 225–37.

Stamatakis, A. (2014). RAxML version 8: a tool for phylogenetic analysis and post-analysis of large phylogenies. *Bioinformatics*, *30*(9), 1312–1313. t

Starrett, J., Derkarabetian, S., Hedin, M., Bryson, R. W., McCormack, J. E., & Faircloth, B. C. (2017). High phylogenetic utility of an ultraconserved element probe set designed for Arachnida. *Molecular Ecology Resources*, *17*(4), 812–823.

Starrett, J., & Hedin, M. (2007). Multilocus genealogies reveal multiple cryptic species and biogeographical complexity in the California turret spider Antrodiaetus riversi (Mygalomorphae, Antrodiaetidae). *Molecular Ecology*, *16*(3), 583–604.

Stockman, A. K., & Bond, J. E. (2007). Delimiting cohesion species: Extreme population structuring and the role of ecological interchangeability. *Molecular Ecology*, *16*(16), 3374–3392.

Sukumaran, J., & Knowles, L. L. (2017). Multispecies coalescent delimits structure, not species. *Proceedings of the National Academy of Sciences*, *114*(7), 1607–1612.

Supple, M. A., Papa, R., Hines, H. M., McMillan, W. O., & Counterman, B. A. (2015). Divergence with gene flow across a speciation continuum of Heliconius butterflies. *BMC Evolutionary Biology*, *15*(1), 204.

Takahata, N., & Slatkin, M. (1990). Genealogy of Neutral Genes in Two Partially Isolated Populations. *Theoretical Population Biology*, *38*, 331–350.

Team, R. C. (2015). R: a language and environment for statistical computing. Vienna, Austria; 2015. *R Foundation for Statistical Computing, Vienna, Austria*. Retrieved from https://www.r-project.org/

Thulin, M., Thiede, J., & Liede-Schumann, S. (2012). Phylogeny and taxonomy of Tribulocarpus (Aizoaceae): A paraphyletic species and an adaptive shift from zoochorous trample burrs to anemochorous nuts. *Taxon*, *61*(1), 55–66.

Vu, V. Q. (2011). ggbiplot: A ggplot2 based biplot. R Packag version 0.55. http://github.com/vqv/ggbiplot.

Warren, D. L., Glor, R. E., & Turelli, M. (2010). ENMTools: a toolbox for comparative studies of environmental niche models. *Ecography*, *33*(3), 607–611.

Warren, D. L., & Seifert, S. N. (2011). Ecological niche modeling in Maxent: the importance of model complexity and the performance of model selection criteria. *Ecological Applications*, *21*(2), 335–342.

World Spider Catalog. (2017). World Spider Catalog. Natural History Museum Bern, online at http://wsc.nmbe.ch, version 18.5, accessed on 11/27/2017.

Xu, X., Xu, C., Li, F., Dinh-Sac, P., & Li, D. (2017). Trapdoor spiders of the genus Cyclocosmia Ausserer, 1871 from China and Vietnam (Araneae, Ctenizidae). *ZooKeys*, *643*, 75–85.

Yang, Z. (2015). The BPP program for species tree estimation and species delimitation. *Current Zoology*, *61*(5), 854–865.

Zhang, C., Zhang, D.-X., Zhu, T., & Yang, Z. (2011). Evaluation of a Bayesian coalescent method of species delimitation. *Systematic Biology*, *60*(6), 747–761.

Figure 1. Comparison of abdominal truncation in *Cyclocosmia truncata* (left, from Sewanee, TN) and *C. torreya* (right, from Torreya State Park, FL).
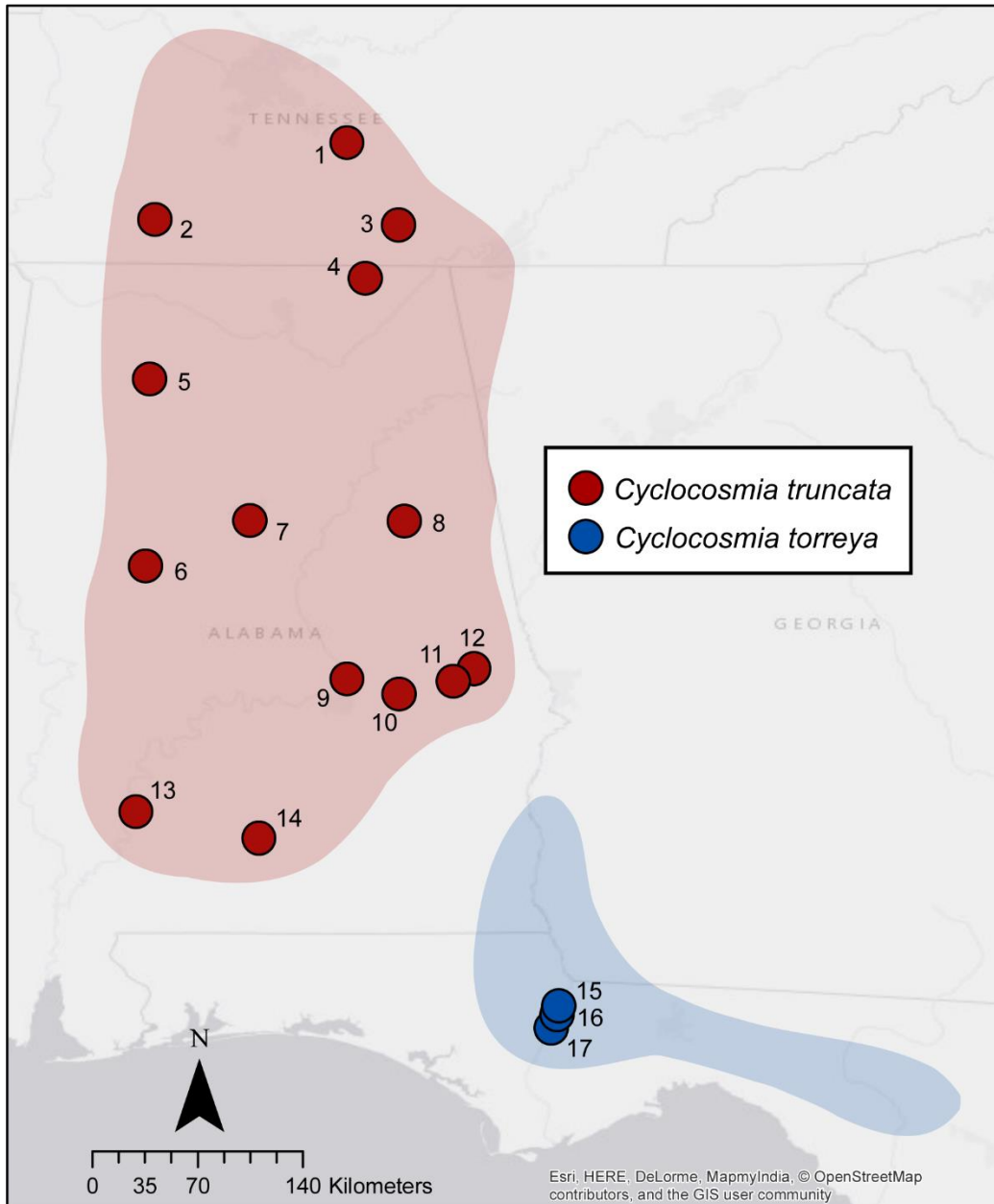
Figure 2. Map of localities of Cyclocosmia specimens used in molecular analysis. Numbers indicate locality and can be found in sample table. Lighter red and blue show the putative species distributions based on historical and modern collections.
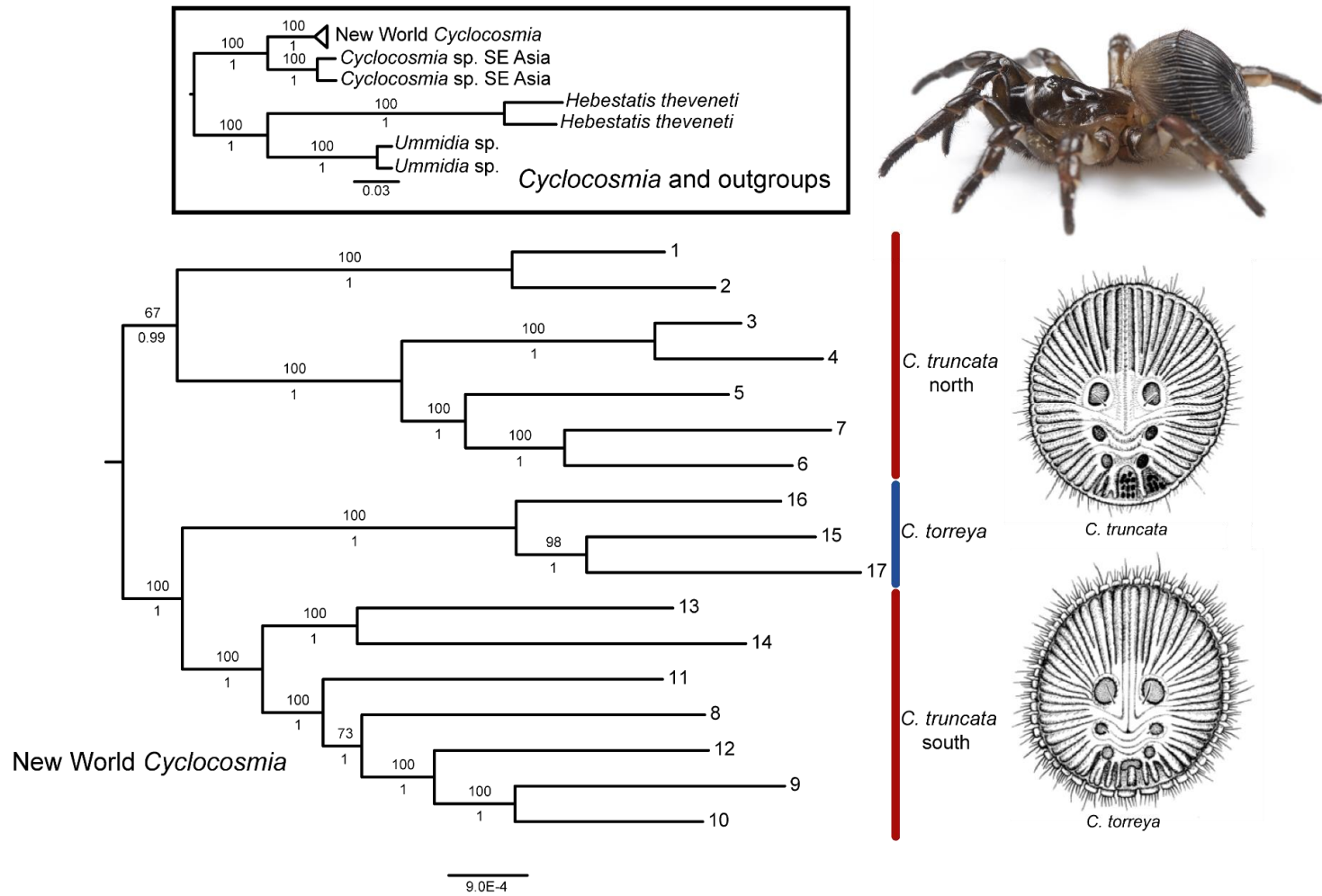
Figure 3. Maximum likelihood and Bayesian inference results, based on a concatenated dataset. Values above branches are maximum likelihood bootstrap support and values below branches are Bayesian posterior probabilities, presented on RAxML tree. Box contains all results with New Word *Cyclocosmia* collapsed. The remainder of the figure is New World *Cyclocosmia* expanded. Numbers on tips correspond to localities in Table 1 and points on map in Figure 2. Abdomen diagrams taken from Gertsch & Platnick (1975).
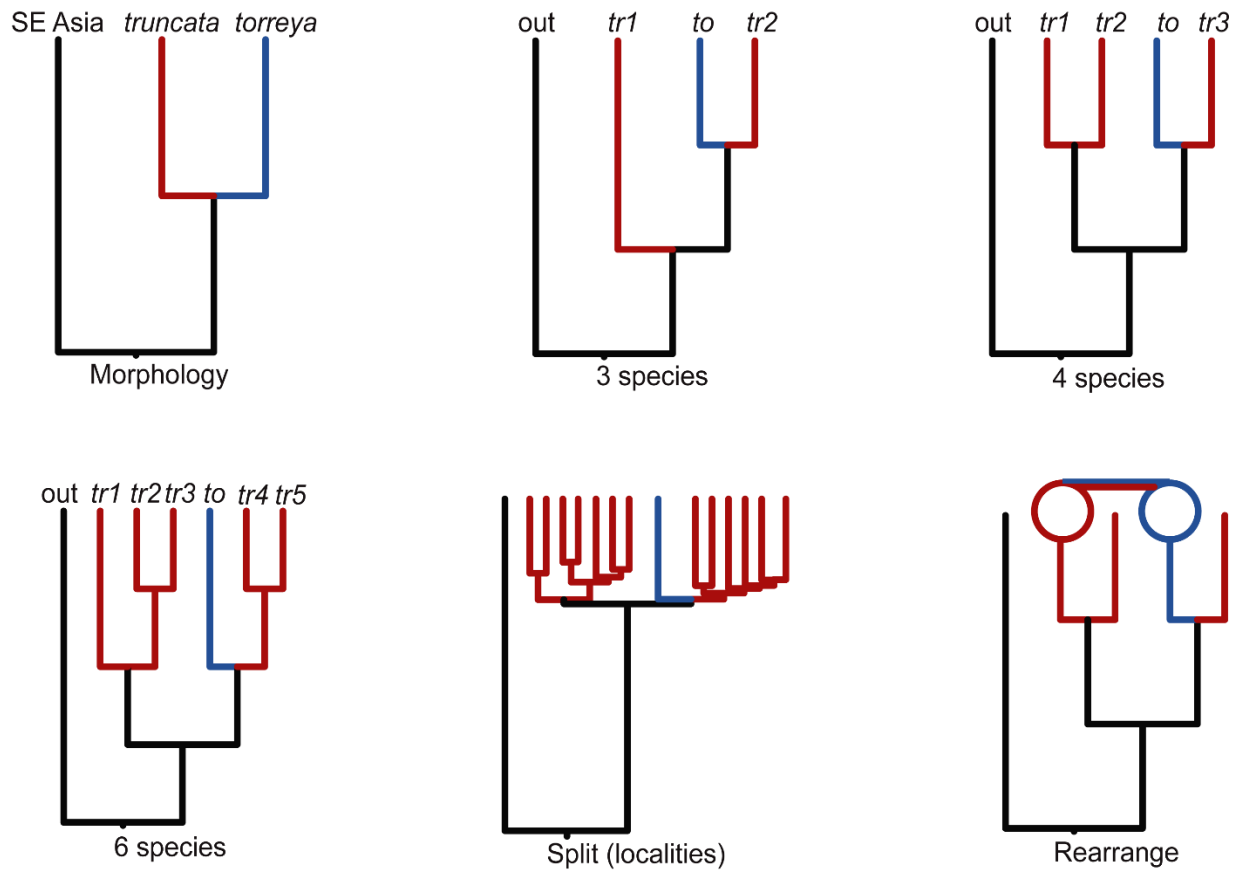
Figure 4. The six species delimitation models are shown as phylogenetic trees, based on anchored enrichment sequences. Red indicates *C. truncata* lineages and blue indicates *C. torreya* lineages.

a)
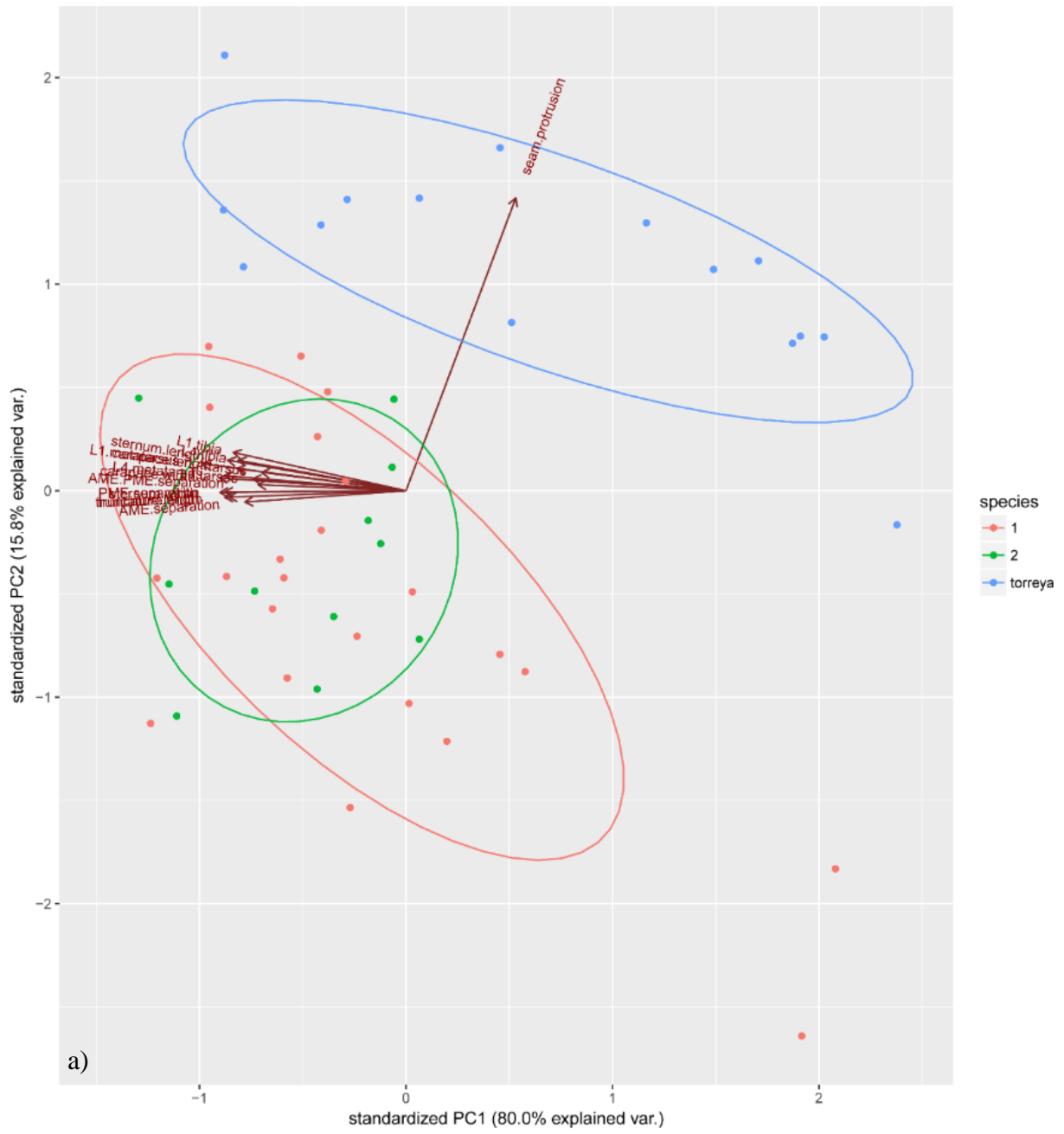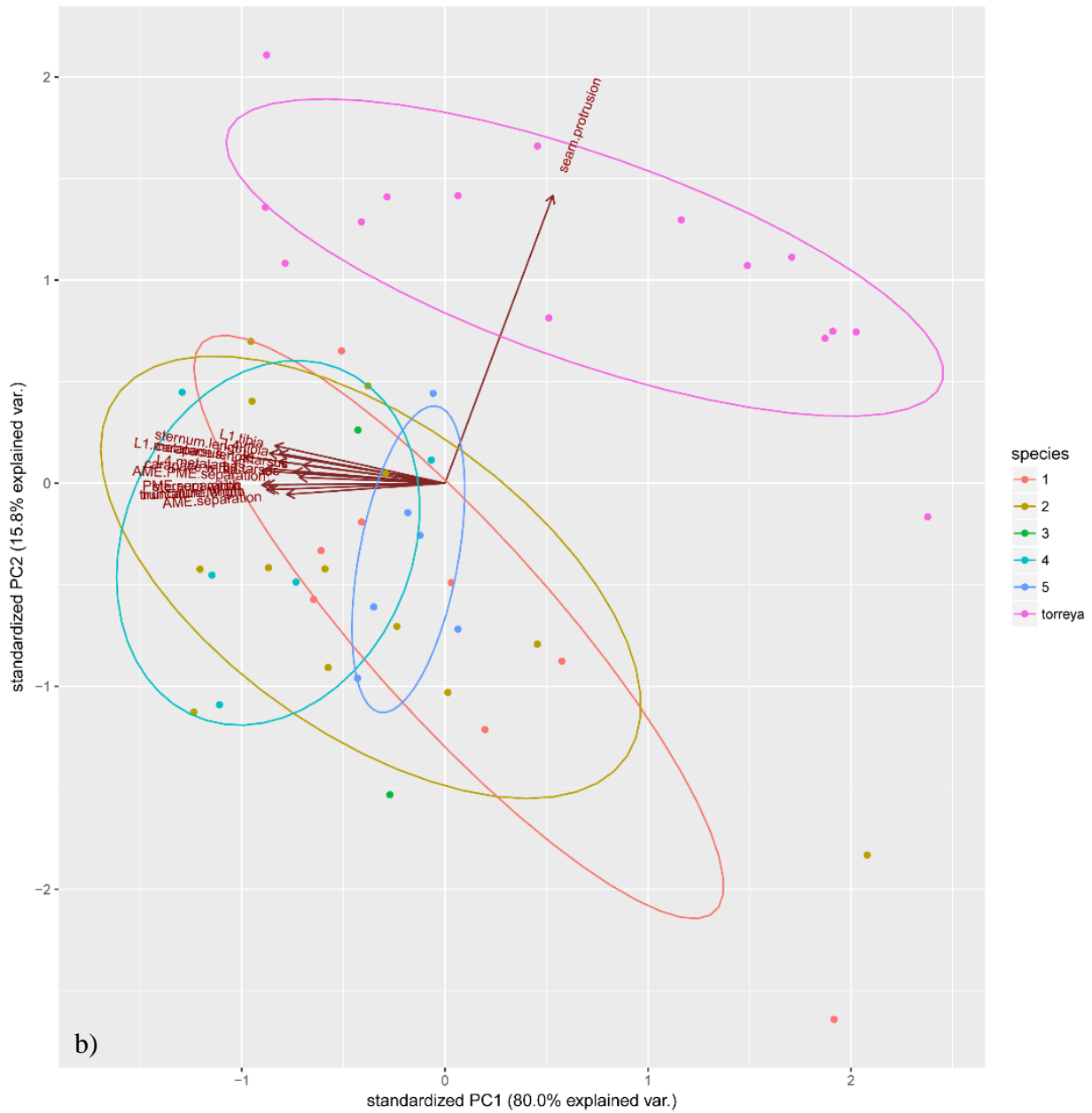
Figure 5. Principal components analysis comparing the groups in the a) three species hypothesis and b) six species hypothesis. Each shape/color corresponds to a putative species group for eavh hypothesis.

33
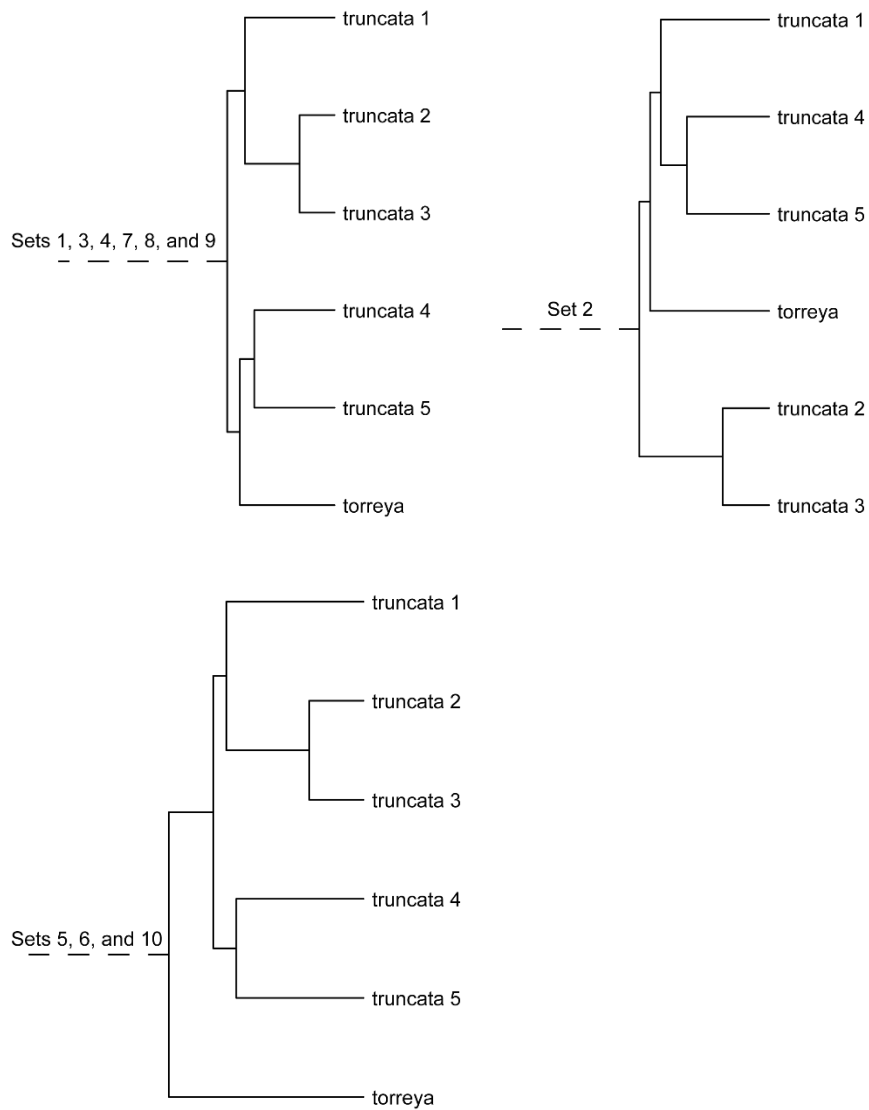
Figure 6. Species trees from the *Beast analyses, based on ten sets of 50 loci, for the most likely species delimitation model (6 species hypothesis). Sets with identical topologies are shown together. Posterior probabilities for individual sets can be found in Appendix 2.
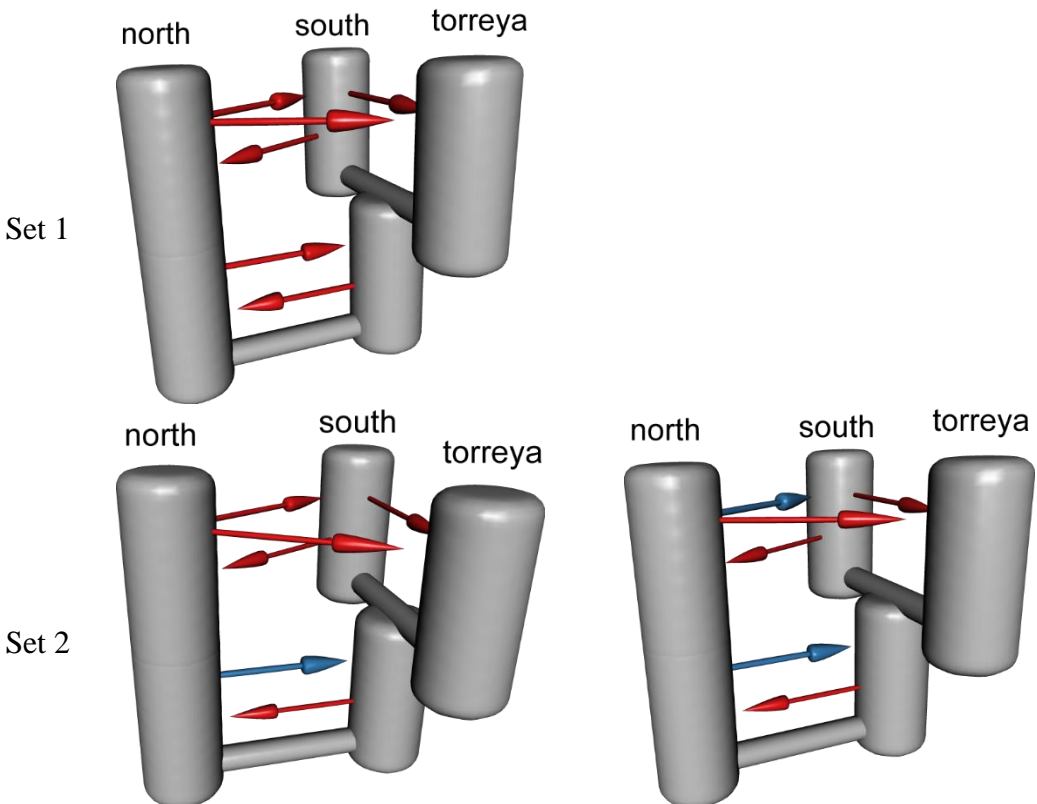
Figure 7. Visualization of demographic models that received the highest or second highest wAIC values in PHRAPL, with blue and red arrows representing presence of gene flow. The model for Set 1 was the highest supported when 768 asymmetric migration with one possible migration rate were explored. The models for Set 2 were the highest supported when a subset of 45 asymmetric models with two possible migration rates were explored. Blue arrows in the set two models indicate a higher rate of gene flow than the red arrows.

3 species hypothesis

6 species hypothesis
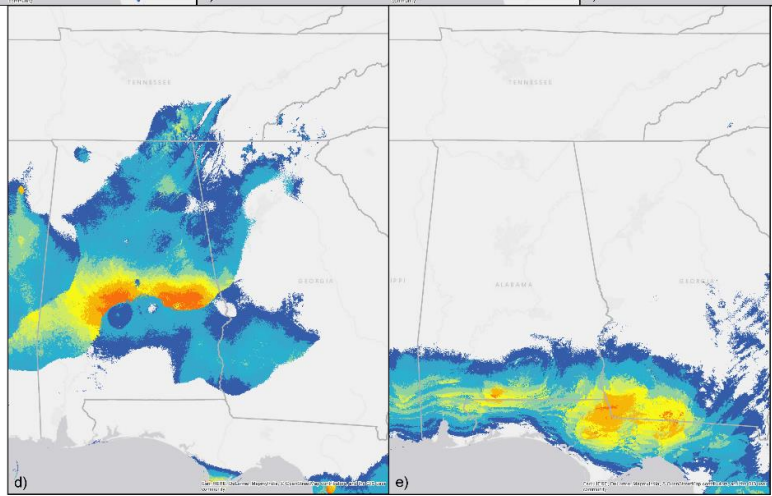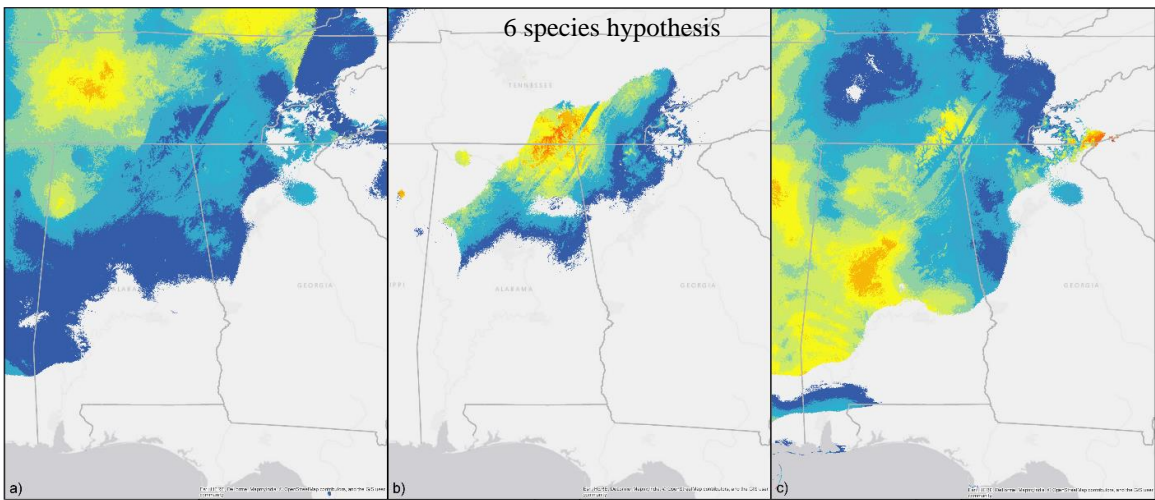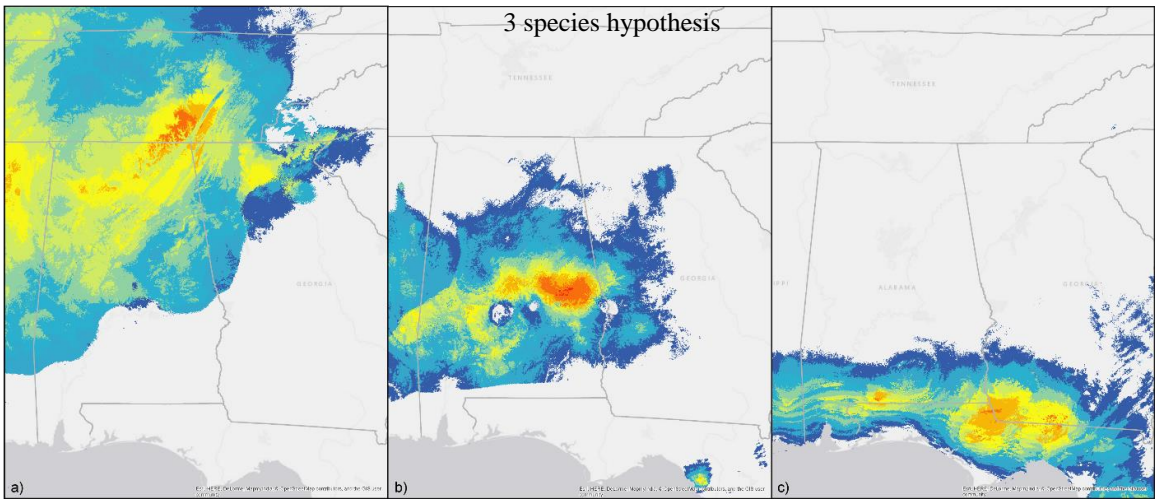
Figure 8. Predicted distributions in the southeast United States for three species hypothesis and 6 species hypothesis. Top maps 3 species hypothesis: a) north *C. truncata* clade, b) south *C. truncata* clade, and c) *C. torreya*. Bottom maps are six species hypothesis: a) truncata 1, b) truncata 2, c) truncata 3, d) truncata 4, and e) *C. torreya*. Group truncata 5 is not included because there were too few locality points to be included in the analysis. Warmer colors indicate higher probability of occurrence and cooler colors indicate a lower probability of occurrence. Areas with < 10% probability of occurrence – color not shown.

Table 1. A list of specimens sequenced for this project and the corresponding localities.

Morphological Species	BFD Species	PHRAPL Clade	Map Number	Voucher No.	Locality	County	State	Country	Latitude	Longitude
New World *Cyclocosmia*										
Cyclocosmia truncata	truncata 1	north	1	AUMS16664	Christiana	Cannon	Tennessee	United States	35.7229	-86.2141
Cyclocosmia truncata	truncata 1	north	2	MY2800	David Crockett State Park	Lawrence	Tennessee	United States	35.2625	-87.3621
Cyclocosmia truncata	truncata 2	north	3	AUMS16182	Sewanee	Franklin	Tennessee	United States	35.2329	-85.9074
Cyclocosmia truncata	truncata 2	north	4	AUMS16346	Skyline Wildlife Management Area	Jackson	Alabama	United States	34.9133	-86.1043
Cyclocosmia truncata	truncata 3	north	5	MY2033	Bankhead National Forest	Lawrence	Alabama	United States	34.3095	-87.3943
Cyclocosmia truncata	truncata 3	north	6	AUMS557	Hurricane Creek	Tuscaloosa	Alabama	United States	33.1931	-87.4188
Cyclocosmia truncata	truncata 3	north	7	AUMS556	Samford	Jefferrson	Alabama	United States	33.4644	-86.7930
Cyclocosmia truncata	truncata 4	south	8	MY2797	Talladega National Forest	Clay	Alabama	United States	33.4596	-85.8735
Cyclocosmia truncata	truncata 4	south	9	AUMS16352	Wetumpka	Elmore	Alabama	United States	32.5169	-86.2130
Cyclocosmia truncata	truncata 4	south	10	AUMS722	EV Smith Research Station	Macon	Alabama	United States	32.4254	-85.9025
Cyclocosmia truncata	truncata 4	south	11	AUMS717	Tuskegee National Forest	Macon	Alabama	United States	32.5039	-85.5784
Cyclocosmia truncata	truncata 4	south	12	AUMS120	Auburn	Lee	Alabama	United States	32.5786	-85.4543
Cyclocosmia truncata	truncata 5	south	13	AUMS5137	Haines Island	Monroe	Alabama	United States	31.7229	-87.4739
Cyclocosmia truncata	truncata 5	south	14	MY2533	McKenzie	Butler	Alabama	United States	31.5663	-86.7402
Cyclocosmia torreya	torreya	torreya	15	AUMS16222	Torreya State Park	Liberty	Florida	United States	30.5649	-84.9510
Cyclocosmia torreya	torreya	torreya	16	MY2577	Bristol	Liberty	Florida	United States	30.5107	-84.9598
Cyclocosmia torreya	torreya	torreya	17	MY2574	Apalachiola River	Liberty	Florida	United States	30.4318	-84.9938
Outgroups										
Cyclocosmia sp.				AUMS791				China	35.8616	104.1953
Cyclocosmia sp.				AUMS2143	Chiang Mai			Thailand	13.8933	98.9169
Hebestatis theveneti				MY2635	near Pinnacles National Monument	San Bentio	California	United States	36.4323	-121.2275
Hebestatis theveneti				MY3741	Hemigo Flats	Los Angeles	California	United States	34.1925	-118.0899
Ummidia sp.				AUMS0588	Eagle Creek	Tallapoosa	Alabama	United States	32.9478	-85.7135
Ummidia sp.				AUMS15478	Andalusia			Spain	36.1336	-5.6982

Table 2. Marginal likelihood estimates and Bayes factors for species delimitation models. The highest performing model and its associated marginal likelihood score are indicated in bold, and received a Bayes factor of N/A.

Hypothesis	Set 1		Set 2		Set 3		Set 4		Set 5	
	MLE	Bayes factor	MLE	Bayes factor	MLE	Bayes factor	MLE	Bayes factor	MLE	Bayes factor
morphology	-74425	2336	-75410	2353	-72187	2105	-74926	2401	-77039	2284
3 species	-73752	990	-74867	1268	-71762	1254	-74335	1219	-76508	1220
4 species	-73526	537	-74558	649	-71382	592	-73991	532	-76161	526
6 species	**-73257**	**N/A**	**-74233**	**N/A**	**-71135**	**N/A**	**-73725**	**N/A**	**-75898**	**N/A**
14 species (localities)	-73311	107	-74684	901	-71748	1227	-74371	1175	-76588	1381
anomalous arrangement	-73750	986	-74818	1169	-71746	1223	-74274	1118	-76423	1050

Hypothesis	Set 6		Set 7		Set 8		Set 9		Set 10	
	MLE	Bayes factor	MLE	Bayes factor	MLE	Bayes factor	MLE	Bayes factor	MLE	Bayes factor
morphology	-73746	2204	-70183	2280	-77903	2290	-76945	2415	-70985	2334
3 species	-73162	1035	-69540	994	-77298	1080	-76321	1166	-70391	604
4 species	-72953	617	-69337	588	-76947	379	-76022	569	-70089	542
6 species	**-72644**	**N/A**	**-69043**	**N/A**	**-76758**	**N/A**	**-75738**	**N/A**	**-69818**	**N/A**
14 species (localities)	-73458	1627	-69694	1302	-77396	1276	-76386	1297	-70444	1253
anomalous arrangement	-73173	1058	-69652	1218	-77291	1066	-76309	1142	-70343	1051

Table 3. Pairwise assessment of niche interchangeability among the 3 species hypothesis clades and 6 species hypothesis groups (group truncata 5 is not included because there were too few locality points to be included in the analysis). Top is niche identity and bottom is p-value. Niche identity is niche overlap results between pairs of species measured by relative ranks metrics (RR): values near 1.0 are considered identical or highly interchangeable. To calculate the p-values, the observed similarity was compared to the null distribution by a one-tailed nonparametric test. The simulated mean is the result of niche identity test conducted on 100 pseudoreplicates of randomized pairs of taxa.

	north	south	torreya
north	-	0.577	0.223
south	<0.01	-	0.575
torreya	<0.01	<0.02	-

	truncata 1	truncata 2	truncata 3	truncata 4	torreya
truncata 1	-	0.713	0.689	0.455	0.150
truncata 2	<0.03	-	0.728	0.664	0.240
truncata 3	<0.04	<0.01	-	0.683	0.335
truncata 4	<0.01	<0.01	<0.01	-	0.516
torreya	**<0.10**	<0.01	<0.01	<0.01	-

Appendix 1
List of specimens and measurements included in PCA.
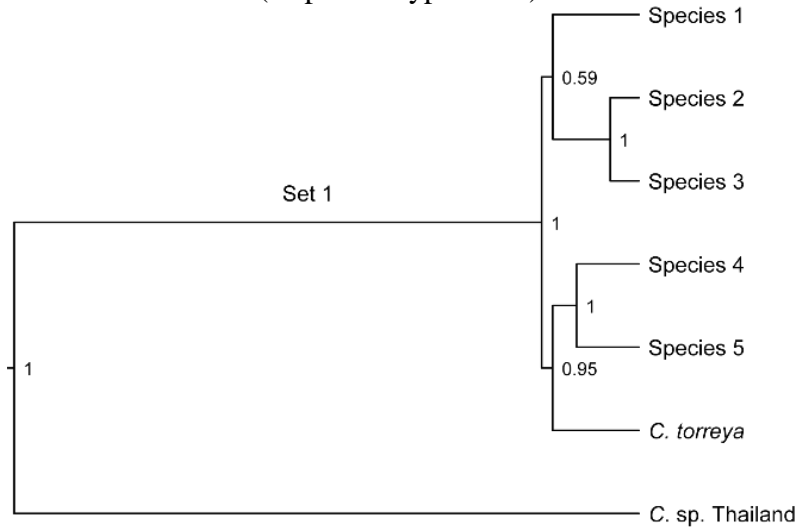
Specimen	3 species	6 species	carapace length	carapace width	PME	AME	AME-PME	sternum length	sternum width	L1 tibia	L1 metatarsus	L1 tarsus	L4 tibia	L4 metatarsus	L4 tarsus	truncature length
AUMS16664	north	1	7.609	7.726	1.311	0.555	0.664	5.364	4.945	3.122	2.826	1.621		3.715	2.196	11.718
AUMS16665	north	1	6.788	6.675	1.171	0.486	0.621	4.569	4.366	2.649	2.443	1.519	2.649	2.272	1.918	9.398
CYC23	north	1	4.655	4.598	0.843	0.41	0.422	2.984	2.905	1.746	1.429	1.062		1.557	1.469	6.518
CYC38	north	1	8.28	7.867	1.37	0.623	0.637	5.317	5.221	3.235	2.913	1.724		2.815	2.331	12.169
CYC39	north	1	7.909	7.848	1.354	0.624	0.588	5.423	4.959	3.265	2.912	1.917		2.865	2.408	11.803
CYC43a	north	1	7.254	7.215	1.2	0.552	0.529	4.548	4.522	2.901	2.506	1.609		2.477	2.124	10.155
CYC43b	north	1	9.127	7.907	1.405	0.631	0.681	5.365	5.347	3.132	2.964	1.761		2.788	2.274	11.705
MY2800	north	1	6.333	6.407	1.025	0.482	0.545	4.305	4.031	2.614	2.168	1.478		2.533	1.812	9.106
AUMS16181	north	1	8.671	7.81	1.324	0.584	0.721	5.522	5.233	3.313	2.853	1.789		3.711	2.475	11.546
AUMS16182	north	2	4.461	4.18	0.744	0.382	0.416	3.088	2.768	1.802	1.431	1.083		1.538	1.426	6.275
AUMS16345	north	2	6.391	6.192	1.166	0.524	0.589	4.386	3.943	2.442	2.234	1.457		2.184	1.93	8.979
AUMS16346	north	2	7.34	6.93	1.221	0.533	0.63	4.733	4.468	2.777	2.44	1.486		2.298	2.091	9.931
AUMS19543	north	2	9.43	8.947	1.605	0.788	0.63	6.174	6.075	3.933	3.427	2.027		4.198	2.46	12.274
CYC25a	north	2	8.606	8.34	1.286	0.709	0.714	5.899	5.218	3.042	2.803	1.736		2.993	2.391	11.149
CYC25b	north	2	8.509	7.565	1.203	0.693	0.693	5.495	5.018	3.107	2.803	1.736		2.643	2.391	10.742
CYC26	north	2	9.696	8.855	1.7	0.767	0.773	6.615	5.89	3.682	3.411	1.88		3.643	2.588	13.069
CYC28	north	2	7.832	7.71	1.232	0.545	0.632	5.448	4.942	3.149	2.714	1.596		2.721	2.226	10.553
CYC32	north	2	8.036	7.824	1.261	0.603	0.639	5.489	5.069	3.205	2.824	1.731		2.511	2.22	11.192
CYC35	north	2	8.152	7.569	1.295	0.564	0.616	5.232	4.927	2.975	2.714	1.636		2.271	2.109	10.254
CYC36	north	2	9.256	8.809	1.561	0.672	0.758	6.339	5.735	3.422	3.171	1.875	3.08	3.457	2.376	12.261
CYC41	north	2	9.141	8.908	1.567	0.707	0.733	5.711	5.018	3.197	2.879	1.902		4.07	2.408	12.721
AUMS1110	north	3	8.014	6.958	1.437	0.512	0.758	4.813	4.314	3.166	2.518	1.615		3.298	2.19	9.869
CYC20	north	3	8.626	7.309	1.346	0.597	0.63	5.483	4.736	2.958	2.958	1.723		2.701	2.608	10.095
AUMS16250	south	4	9.124	8.997	1.362	0.613	0.683	6.193	5.626	3.39	3.39	1.963		3.279	2.794	13.576
AUMS16399	south	4	7.52	6.933	1.131	0.577	0.631	4.983	4.512	2.485	2.485	1.552		2.642	2.137	10.748
AUMS173	south	4	9.623	9.523	1.65	0.753	0.804	6.373	5.912	3.768	3.681	2.022		4.385	2.559	13.116
AUMS717	south	4	8.662	8.885	1.608	0.784	0.803	6.054	5.55	3.607	3.163	1.84	3.031	4.247	2.23	12.152
AUMS7605	south	4	8.711	7.918	1.396	0.622	0.715	5.58	5.449	3.617	2.879	1.781		3.594	2.299	10.819
AUMS5136	south	5	7.665	7.016	1.213	0.497	0.632	5.128	4.525	3.208	2.68	1.603		3.376	2.074	10.738
AUMS5137	south	5	7.926	7.117	1.198	0.455	0.636	4.688	4.688	3.087	2.794	1.62		3.404	1.956	10.715
MY2532	south	5	8.123	7.373	1.317	0.601	0.677	5.554	4.688	3.422	2.868	1.791		3.686	2.275	10.542
MY2533	south	5	7.813	7.218	1.257	0.469	0.628	5.271	4.568	3.329	2.81	1.667		3.449	2.249	10.446
MY2534	south	5	7.977	7.222	1.35	0.549	0.65	5.178	4.527	3.322	2.78	1.703		3.584	2.342	9.8
MY2535	south	5	6.989	6.623	1.33	0.571	0.623	4.79	4.169	2.878	2.494	1.487		3.239	1.942	10.446
AUMS16221	torreya	torreya	5.399	4.558	0.801	0.406	0.459	3.416	2.905	1.993	1.557	1.159		1.719	1.53	6.387
AUMS16222	torreya	torreya	5.154	4.522	0.785	0.38	0.428	3.282	2.944	1.945	1.588	1.142		1.642	1.483	6.322
AUMS16223	torreya	torreya	5.641	4.845	0.81	0.383	0.459	3.686	3.077	1.762	1.588	1.135		1.7	1.629	7.062
AUMS16224	torreya	torreya	5.132	4.702	0.752	0.384	0.443	3.271	2.877	1.705	1.508	1.155		2.35	1.578	6.926
CYC10	torreya	torreya	7.134	6.309	1.17	0.482	0.631	4.722	3.803	2.496	2.171	1.381		3.112	2.082	8.891
CYC11	torreya	torreya	9.431	8.604	1.472	0.648	0.798	6.466	5.351	3.253	3.054	1.98		4.311	2.592	10.927
CYC13a	torreya	torreya	8.707	8.965	1.51	0.634	0.68	6.301	5.238	3.895	3.428	1.9		4.226	2.66	10.981
CYC13b	torreya	torreya	9.084	8.487	1.501	0.687	0.627	6.181	4.932	3.834	3.332	1.965	2.837	3.855	2.512	11.381
CYC13c	torreya	torreya	5.716	5.027	0.896	0.403	0.488	3.854	3.235	2.284	1.861	1.16		2.407	1.573	7.083
CYC14	torreya	torreya	7.119	6.358	1.04	0.443	0.562	4.562	3.91	2.76	2.362	1.499		3.06	2.053	8.522
CYC17	torreya	torreya	5.877	5.375	0.892	0.446	0.476	3.912	3.27	1.9	1.9	1.326		2.483	1.789	7.461
CYC18a	torreya	torreya	7.887	7.002	1.202	0.479	0.691	5.362	4.326	3.045	2.689	1.619		3.299	2.148	9.253
CYC18b	torreya	torreya	8.484	7.638	1.444	0.576	0.757	5.662	4.701	3.464	2.925	1.731		3.625	2.235	10.465
CYC45	torreya	torreya	8.127	8.052	1.241	0.525	0.677	5.723	4.846	3.363	2.776	1.665		3.432	2.337	10.24
CYC8	torreya	torreya	4.484	3.848	0.756	0.353	0.4	2.878	2.571	1.776	1.456	0.987		1.937	1.368	6.177

Table continued.

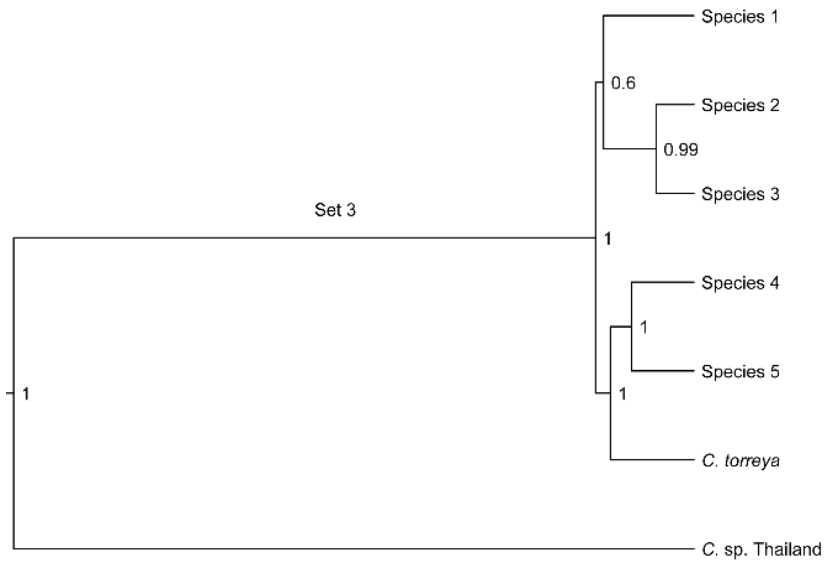| truncature width	margin protrusion
11.418	0.137
9.322	0.102
6.235	0.078
12.56	0.128
11.431	0.183
9.948	0.13
11.261	0.116
9.299	0.123
10.926	0.122
6.113	0.105
8.408	0.124
9.837	0.107
11.881	0.087
10.673	0.102
11.444	0.116
12.851	0.115
10.66	0.149
10.747	0.175
10.037	0.116
12.125	0.176
12.843	0.162
9.991	0.084
9.494	0.155
13.369	0.11
10.344	0.159
12.983	0.154
11.792	0.091
11.536	0.117
10.743	0.137
10.341	0.177
10.059	0.102
10.091	0.139
9.719	0.115
9.667	0.121
6.047	0.258
5.982	0.262
6.838	0.286
6.906	0.256
8.526	0.292
10.621	0.284
10.958	0.216
11.367	0.202
6.913	0.272
8.124	0.213
7.416	0.275
8.814	0.25
9.915	0.228
10.31	0.24
5.885	0.199

Appendix 2

Results of the *Beast analyses, based on ten sets of 50 loci, for the most likely species delimitation model (6 species hypothesis). Values at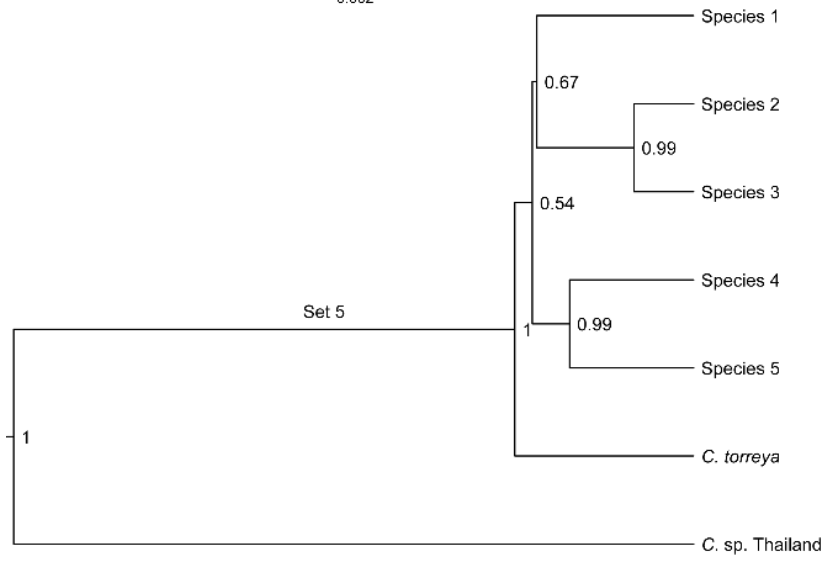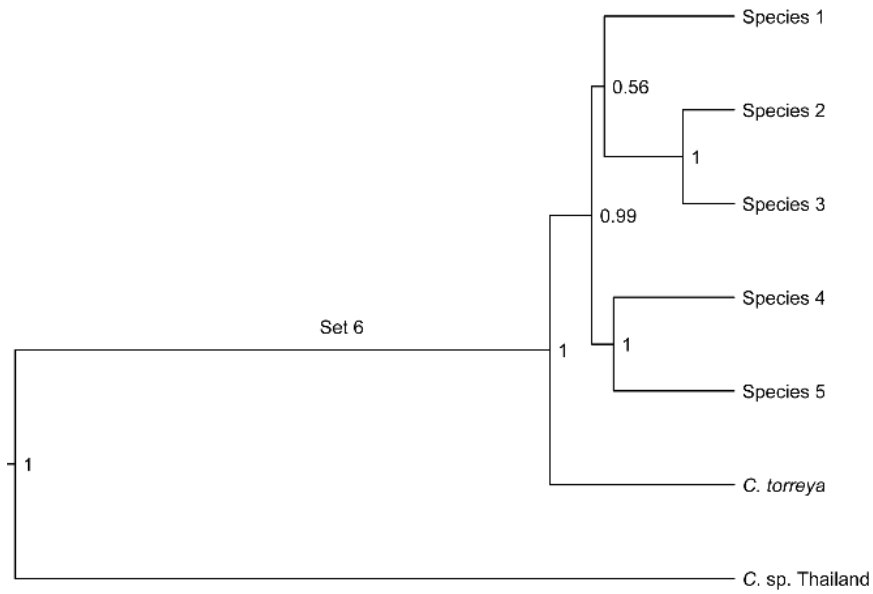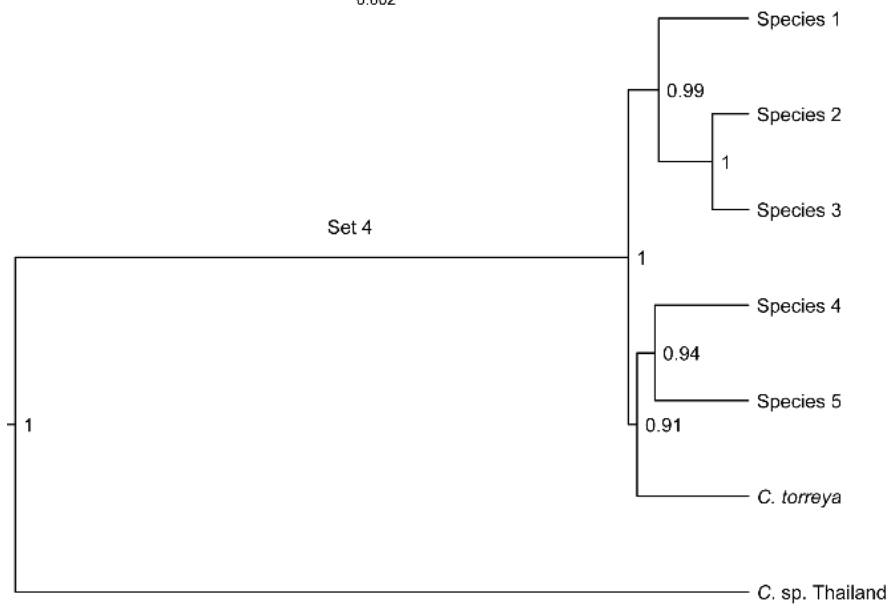 nodes are posterior probabilities.